



Multifold increase in dye adsorption by nanoparticles of a nanobiocomposite through its controlled simultaneous synthesis with simultaneous adsorption and photodegradation

Roohan Rakhshae¹ · Nasim Ertegha¹

Received: 5 December 2023 / Accepted: 23 January 2024 / Published online: 7 March 2024
© The Author(s) 2024

Abstract

It was shown for the first time that the efficiency of dye adsorption by nanoparticles (NPs) in a cheap and safe nanobiocomposite was increased several times (713%) due to the synchronization of the controlled synthesis of nanobiocomposite (α -Fe₂O₃NPs/lemon peel (LP)/Fe₃O₄NPs) in the final stages of its nanoparticles growth with the removal process of Brilliance Green, compared to that of the separate synthesis from the removal process. It was only performed during the simultaneous adsorption and photodegradation (SAP) because of the stabilization of its NPs by the small substances obtained from dye photodegradation, unlike alone adsorption (AA) with agglomeration of its NPs. It turned out that only in the case of simultaneous nanobiocomposite synthesis with dye removal process during SAP, the percentage of dye adsorption by nanoparticles of nanobiocomposite is higher than that of organic substances of its LP. A competitive process was happened between NPs and the organic substances of LP in nanobiocomposite including hydrolyzable tannin, cellulose and effective alcohols, in the absence of performance of pectin at pH = 6.0 and, with participation of only pectin at pH = 4.0, for adsorption with and without photodegradation of the dye which was studied by reaching the quantitative values and the mass balances.

Keywords Simultaneous removal and synthesis · Nanoparticles stabilization and agglomeration · Simultaneous adsorption and photodegradation · Dye · Mass balances

Introduction

It is noticeable that tri-phenyl-methane (TPM) dyes, as an important kind of commercial ones, have various applications in industries (Duxbury 1993). Among the TPM dyes, Brilliant Green (BG) has variety uses (usually with other TPM dyes, such as malachite green and crystal violet) in the textile industry to color silk, wool, leather, cotton and paper. It is also widely used in fish farming industry because of its antimicrobial, anti-parasitic and antifungal spectrum, low cost and high efficiency in the prevention and treatment of certain fish diseases (Eshaghi and Ahmadi 2011). The main reason for removing BG dye is the toxicity with mutagenic and carcinogenic effects that can influence both aquatic biota and humans (Seshadri et al. 1994). There are many various

technologies have been used for dye removal over the years, some of the traditional techniques for color removal are, activated carbon (charcoal), filtration and coagulation that each method has a few advantages and disadvantages (Toor 2006).

Among the new techniques, adsorption has a particular role in practical applications because of its simplicity and cost effectiveness. In addition, there are several advanced oxidation processes being evaluated for the destruction of dyes. The photocatalysis degradation such as the effective UV light can be a kind of this method which consider in this study (Toor 2006; Yagub et al. 2014).

Fe₃O₄ nanoparticles which are in focus as important dye adsorbents cause their large specific surface area and small diffusion resistance that has kinds of ways for preparing and the one that is considered in this study it is co-preparation way. Also, α -Fe₂O₃ is the other magnetic metal oxides which is extremely studied materials extensively used as catalysts, sensors, fine ceramics, data storage materials and pigments and for preparing, the hydrothermal synthesis method is chosen among the other ways. To avoid

✉ Roohan Rakhshae
roohan_rakhshae@guilan.ac.ir

¹ Department of Chemistry, Faculty of Science, University of Guilan, P.O. Box: 41335-19141, Rasht, Iran

the agglomeration and improve the stability of adsorption in aqueous solution, and even for the connection of nanocomposite' particles, like in this study, the surface with the organic agents can be modified (Mohammadi et al. 2014; Ahmmad 2013).

Lemon peel, like the peel of other citrus fruits as a cheap, safe and available agent, contains cellulose and hemicellulose, tannin, pectin, various alcohols and aliphatic substances, and the presence of functional groups in some of these substances makes them functional (Oboh et al. 2014) which these organic matters can both adsorb dye and bind to the nanoparticles (Rakhshae and Noorani 2017).

Cellulose and pectin are the most structurally complex family of polysaccharides in nature with covalently linked galacturonic acid-rich plant cell wall polysaccharides (Mohen 2008). It can be noticed that the pectin's functional groups such as hydroxyl and carboxylate can play the most role for modifying the surface of nanoparticles and be as the connector in the subjected nanocomposite (Mohammadi et al. 2014). The batch experiments are usually carried out in order to determine the maximum adsorption capacity and the continuous adsorption is most of the time desired from industrial point of view (Ahmad 2010). On the other hand, photodegradation using nanophotocatalysts is used as the effective method to remove dye, but due to the limitations of its removal mechanism, they do not have a very wide range of performance (Rakhshae and Darvazeh 2017 and 2018).

In this study, it is used the batch system for both alone adsorption (AA) and the simultaneous adsorption and photodegradation (SAP) of BG by ($\alpha - \text{Fe}_2\text{O}_3$ NPs/lemonpeel/ Fe_3O_4 NPs) synthesized both simultaneously with the removal process and separately from it. It was shown that the highest dye removal efficiency by the nanobiocomposite occurs when the final stages of its synthesis and the growth of its nanoparticles are simultaneous with the simultaneous adsorption and photodegradation (SAP) due to autocatalysis role of small organic substances resulting from photodegradation in more stabilization and efficiency of its nanoparticles. In this case, about 713% increase in dye adsorption by nanoparticles of nanobiocomposite was observed.

The alone adsorption was also used to determine the contribution of each removal mechanism. The lemon peel (LP) as a matter containing the cellulose and hemicellulose, linalool, borneol, fenchol, hydrolyzable tannin and pectin (the main adsorption factors) was connected to $\alpha - \text{Fe}_2\text{O}_3$ NPs as a photocatalyst and Fe_3O_4 NPs as a connection mediator.

It was shown that the dye degradation products when the process is carried out as SAP can contribute to nanoparticles stabilization and play a role in increasing the contribution of dye removal, while agglomeration of NPs is happened in AA when the nanobiocomposite synthesis is done in its final stages at the same time as the dye removal process.

The mass balance of the adsorbed dye showed that among the organic components of LP in nanocomposite, only the molecules of linalool, borneol, fenchol, cellulose and hydrolyzable tannin can be considered as the only dye adsorption factors at pH = 6.0, while pectin is only agent of LP in nanocomposite to adsorb dye at pH = 4.0. Also, Fe_3O_4 NPs and even $\alpha - \text{Fe}_2\text{O}_3$ NPs can adsorb the part of BG molecules either in alone adsorption or in the simultaneous adsorption and photodegradation process having the adsorbing functional groups.

Materials and methods

The synthesis of ($\alpha - \text{Fe}_2\text{O}_3$ NPs/lemonpeel/ Fe_3O_4 NPs) was carried out both in absence and presence of dye removal processes to evaluate agglomeration and stabilization of its nanoparticles. It was performed in the presence of both only dye molecules (in AA) and smaller components resulting from dye photodegradation (in SAP). The goal is to investigate the effect of smaller materials resulting from photodegradation on the change in size and crowding of nanoparticles at the same time as synthesis, in addition to the usual dye contact of nanocomposite materials after the end of synthesis.

Fe_3O_4 NPs were synthesized with co-precipitation of $\text{FeCl}_3 \cdot 6\text{H}_2\text{O}$ and $\text{FeSO}_4 \cdot 7\text{H}_2\text{O}$ in alkaline solution with the following method. First in a beaker, 6.00 gr $\text{FeCl}_3 \cdot 6\text{H}_2\text{O}$ and 4.0 gr $\text{FeSO}_4 \cdot 7\text{H}_2\text{O}$ were dissolved with 100 ml distilled water by heating up to 90 °C then quickly added 50ml $\text{NH}_4\text{OH} 26\%$ to our solution to make the pH = 10. After that the solution were mixed 30 min at 80°C. The black nanoparticles sediment were washed with distilled water and ethanol 96% then dried at 50 °C. In the next step for the synthesis of $\alpha - \text{Fe}_2\text{O}_3$ (Rakhshae and Darvazeh 2017) and $\alpha - \text{Fe}_2\text{O}_3$ /LP, first, 3.00 gr of lemon peel and 7.40 gr of $\text{Fe}(\text{NO}_3)_3 \cdot 9\text{H}_2\text{O}$ was mixed with 80 ml distilled water at room temperature for 10 min under magnetic stirring. Then was dropped ammonia (76%) into the resultant solution at room temperature till pH = 9.0 and was mixed for 20 min. The solution was transferred to an autoclave which was heated at 70 °C for 5 h under ambient temperature. The autoclave was cooled to room temperature and the product was washed with ethanol (96%) and distilled water then was dried at 50 °C. In the final step, it is chosen two ways for preparing the final composite, first, was prepared the situation for adding 0.25 g magnetite to the solution that consisted of 0.50 g hematite/ LP which mixed with distilled water in 25 °C and was mixed for 10.0 min. This nanocomposite is named NCT as product of P1 (the nanobiocomposite ($\alpha - \text{Fe}_2\text{O}_3$ /lemonpeel/ Fe_3O_4) in optimum form) which is mixed in the last stage of synthesis by heating up to 25 °C). NCT as P1 after collecting by filtration and washing with distilled water for 5.0 min is then contacted with

BG solution for 10.0 min as the removal time (a total of 20.0 min of final mixing time in synthesis of NCT and dye removal, separately). Most of the experimental cases in this study were used 0.05 g of this matter in 10 ml of BG solution (5.0 g/l). In the second way, the last step of synthesis was done at 10 °C which is named NCWT (the nanocomposite (α -Fe₂O₃/lemonpeel/Fe₃O₄) that is synthesized without heating). In the both ways, the result sediment was washed with distilled water and ethanol 96% then dried at 50 °C. α -Fe₂O₃/UV (without lemonpeel/Fe₃O₄) was used to compare the results of BG removal by alone adsorption with the simultaneous photodegradation and adsorption.

If in the other experiment, the total time of 20.0 min of the final mixing in the synthesis of NCT is divided into two 10.0 min, which include the first 10.0 min including the same mixing during the synthesis of NCT (no contact with the dye) and the second 10.0 min including the mixing in contact with the dye solution and in the presence of the synthesis agents (without collecting and washing of NCT before adding dye solution, unlike P1, that is, the simultaneous synthesis during the last 10.0 min with the dye removal process), the NCT is as product of P2. In other words, 10.0 min of the final growth of nanoparticles is done simultaneously with the removal of dye for P2. That is, the contact time of the NCT with the dye for removal in both cases of P1 and P2 is 10 min. In order to evaluate the effect of other simultaneous synthesis and removal times on the average size of nanoparticles in NCT and its ability to remove dye, in addition to 10 min (for P2), times of 2.0, 5.0 and 15.0 min were also examined.

Agglomeration and/or stabilization of NPs during AA and SAP methods, in the separate and simultaneous states of NCT synthesis and dye removal processes for P1 and P2, respectively (using XPS and TEM studies), and the obtained changes of the dye removal values as adsorption on NPs, adsorption of the organic agents of LP and photodegradation by photocatalyst in NCT can be seen. In other words, the effect of large dye molecules and the smaller components resulting from its photodegradation can be investigated on the stabilization and/or agglomeration of nanoparticles of NCT.

Results

The different effects of changing pH on dye removal using P1 and P2 during AA and SAP

pH is also a vital parameter for the reaction performance that affect the size of photocatalyst aggregates, the charge state of the photocatalyst particles and the quantum yield of oxidative/reductive species. It can be noticed that the pH plays an

Table 1 Surface charges of dye and substances in NCT at different pHs. The PZC/pKa values are considered by default for the pure components of the materials that are present in NCT structure that the type of electric charge of the components corresponds to the results

Substances (PZC / pKa of pure components based on various references)	Surface charge in different pHs		
	pH=4.0	pH=6.0	pH=10.0
BG (5.3)	+	-	-
Fe ₃ O ₄ NPs (8.2)	+	+	-
α -Fe ₂ O ₃ NPs (9.3)	+	+	-
Cellulose & Hemicellulose (12.0–12.8)	+	+	+
Alcohols with more amounts (Linalool, Borneol, Fenchol) (14.5 – 15.3)	+	+	+
Tannin (8.5)	+	+	-
Pectin (3.5)	-	-	-

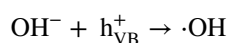
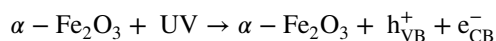
Table 2 Materials from LP (Obboh et al. 2014) of (α -Fe₂O₃ NPs/ LP / Fe₃O₄ NPs) with a negligible effect on BG adsorption

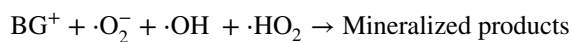
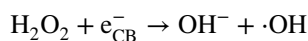
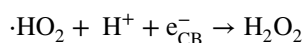
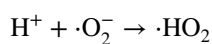
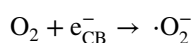
Alcohols with very small amounts	Compounds without effective functional groups to remove BG
Benzyl alcohol	Limonene (with the highest percent)
Nerol	Sabinene
Terpineol	α -Pinene
Myrcene	β -Pinene

important role in the generation of hydroxyl radicals as the main agent to dye degradation. By the effect of adsorption process on degradation ability, the PZC of nanoparticles and pK_a of cationic dye can be played an important rule for the effect of UV light degradation too.

Table 1A shows the surface charges of dye and remover substances in nanobiocomposite (α -Fe₂O₃ NPs/lemon peel (LP)/Fe₃O₄ NPs) as NCT at different pHs due to their point of zero charge (PZC) and pKa. Table 2 shows materials from LP in NCT with a negligible effect on BG adsorption.

The equations of photodegradation by hematite are as follows:





As can be seen, increasing both acidic and alkaline solutions can increase the radicals as the degradation agents of the dye. So that OH^- increases $\cdot\text{OH}$, while H^+ creates $\cdot\text{HO}_2$ and H_2O_2 (which H_2O_2 produced $\cdot\text{OH}$). But as can be seen from Fig. 1(A1) when photodegradation was done with adsorption, simultaneously (SAP) using NCT as P1, only the acidic pHs (of 4.0 and 6.0) increases the dye removal, compared with alone adsorption. As can be seen from Fig. 1(A1), the removal percentage in batch is decreased due to the increase in pH in SAP (unlike that of fixed bed system, in next sections). It shows that the synergistic role of photodegradation with adsorption to remove BG is done only at the acidic pHs, while it was reduced at neutral and alkaline pHs.

The reason can be that at the acidic pHs, increasing H^+ increases $\cdot\text{HO}_2$ (as a main agent of dye degradation) and this radical produces H_2O_2 in the presence of H^+ and that H_2O_2 produces $\cdot\text{OH}$ (as other agent of dye degradation), while at pH of 10.0, although the production of $\cdot\text{OH}$ from OH^- is expected, OH^- can be absorbed by the matter in LP of NCT such as cellulose with higher mass percentage (Rivas et al. 2013) as a main adsorbent which has positive charge at this pH. This case reduces the positive points of cellulose, so the adsorption of the negative dye (at pH of 10.0) is reduced, and therefore, the total dye removal (due to the simultaneous photodegradation and adsorption) is reduced. In other words, the UV-C light acts an inhibitor factor for dye adsorption at pH = 10.0. Figure 1(A1 and A2) shows the effect of pH for simultaneous adsorption and photodegradation process (SAP) and alone adsorption for SAP process for BG removal by NCT as P1 and P2. The factors of free radical and the electric charge between agents cause the BG removal in SAP at pH of 10.0 for P1 to be less than AA process (unlike pHs of 4 and 6). The maximum removal was obtained at pH = 6.0 for P2 during SAP and AA. Figure 1(A3 and A4) shows the effect of the synchronization of NCT with BG removal during the different times on the mean size of NPs of NCT and dye removal efficiency, at pH = 6.0 for AA and SAP processes.

Study of agglomeration and stabilization of nanoparticles in NCT using P2 during AA and SAP processes, respectively, and their effects on decreasing and increasing dye adsorption

Figure 1B–F shows the XPS spectra of bare NCT, NCT-BG after alone adsorption (AA) and NCT-BG after simultaneous adsorption and photodegradation (SAP) for O 1S (H–O and Fe–O), Fe 2P (1/2 and 3/2), C–C and C–O.

As can be seen from Fig. 1B–F (confirmed by TEM images of Fig. 1G–K) in AA and SAP by P2 (simultaneous NCT synthesis and BG removal), agglomeration of NPs (due to the presence of the large BG molecules) and stabilization of NPs (due to the presence of small substances from dye photodegradation) in NCT-BG occur, respectively, compared with those of bare NCT. In both AA and SAP by P1 (separate NCT synthesis and BG removal), no appreciable stabilization and agglomeration for NPs in NCT-BG occur compared with those of bare NCT.

It is possible that when P2 is used in SAP because of both the smaller and more components resulting from the degradation of the dye with various functional groups that have more ability to bind to nanoparticles, due to their greater mobility and permeability, create a better connection with nanoparticles and stabilize them, unlike using P1.

In the simultaneous synthesis with the removal (P2) in AA, due to the lower mobility and penetration of large color molecules, not only the stabilization of nanoparticles is not done, but in the last stage of the growth of nanoparticles, accumulation and agglomeration occur. This is not observed in the use of P1 in AA. The reason can be the role of large color molecules and the crowding resulting from them. In such a way, it causes the proximity of the functional groups of nanoparticles to each other, which creates aggregation and agglomeration.

The presence of free –OH of NCT and the intensity of its peak of XPS decrease further due to the greater binding of dye and substances from its decomposition to nanoparticles and organic substances of LP while intensity of Fe–O and Fe (2P) peaks shows an increase during SAP using P2, which indicates a smaller size (larger surface area) of nanoparticles as a result of their stabilization by the components resulting from the photodegradation of the dye.

In Fig. 1B and D, the proximity of the peaks of Fe–O and Fe (2P) is due to the lack of significant stabilization or agglomeration of NPs in NCT-BG during AA and SAP by using P1 compared with those of bare NCT which was confirmed by TEM. The decrease in the intensity of peaks H–O in NCT-BG of AA and SAP (in Fig. 1B) compared to those of bare NCT is due to the consumption of –OH of nanoparticles and organic materials of LP to absorb the functional groups of the dye,

Fig. 1 The effect of pH for simultaneous adsorption and photodegradation process (SAP) and alone adsorption (AA) by NCT as P1 and P2 in removal time of 10.0 min (A1 and A2) and effect of simultaneous synthesis times with removal process on NPs mean size of NCT and BG removal percentages during SAP and AA at pH = 6.0 (A3 and A4). XPS spectra of bare NCT, NCT-BG after alone adsorption (AA) and NCT-BG after simultaneous adsorption and photodegradation (SAP) (B–G). TEM images of bare NCT (H), NCT-BG using NCT as P1 in SAP and AA (I and J), and NCT-BG using NCT as P2 in SAP and AA (K and L). AA and SAP were done for 2.0 mg BG/g NCT, pH = 6.0, dosage = 0.05 g/ 10 ml, $C_0 = 10$ ppm, $T = 20$ °C

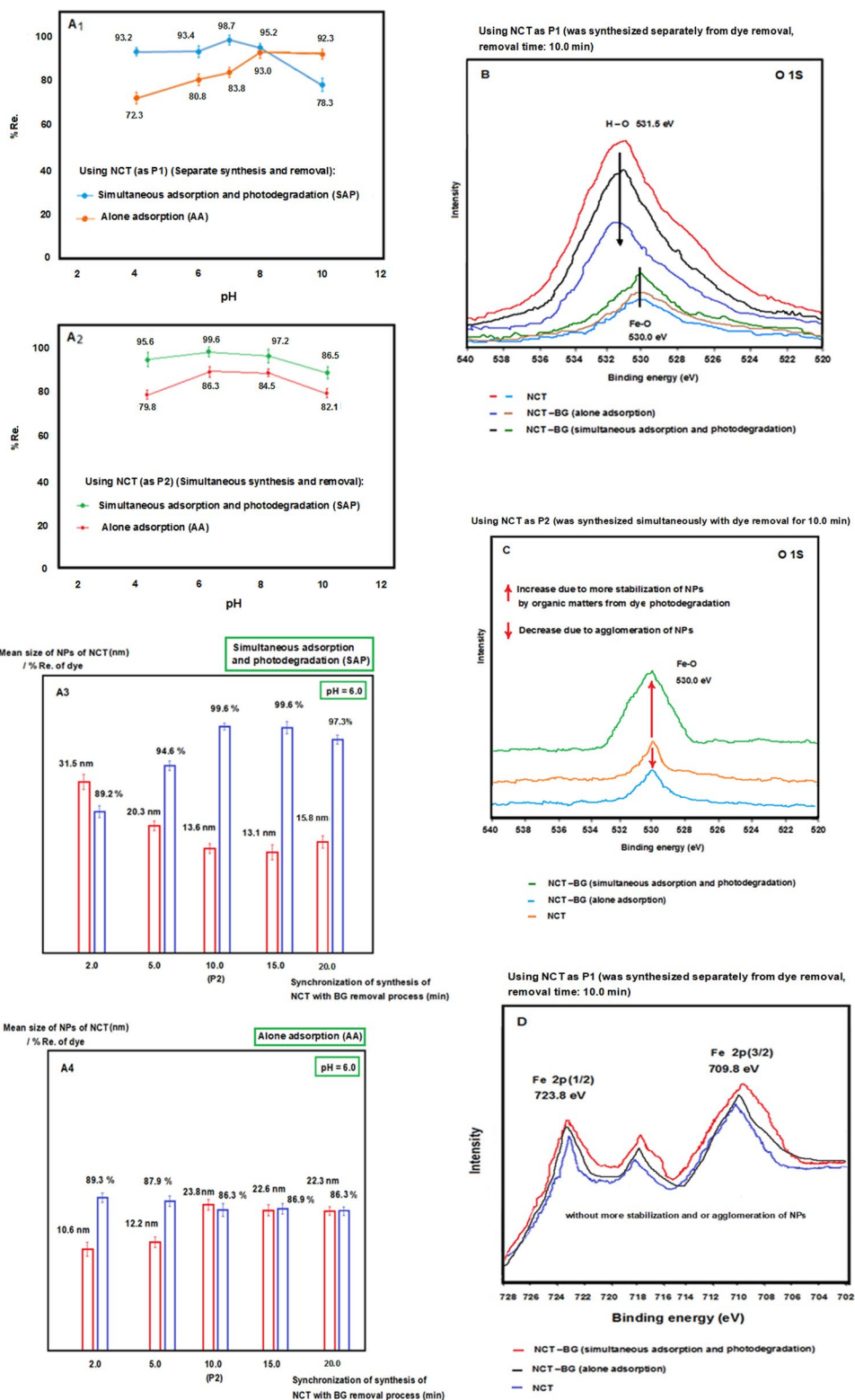
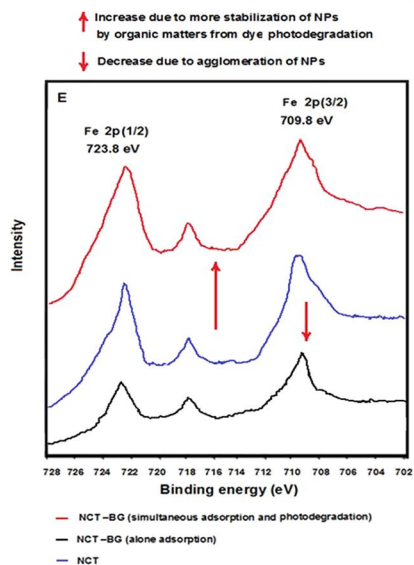
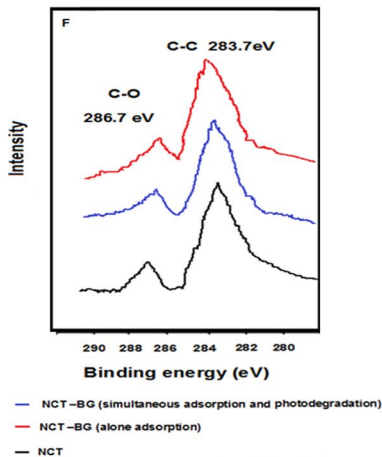


Fig. 1 (continued)

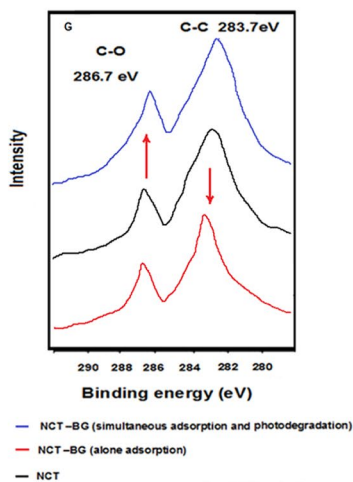
Using NCT as P2 (was synthesized simultaneously with dye removal for 10.0 min)



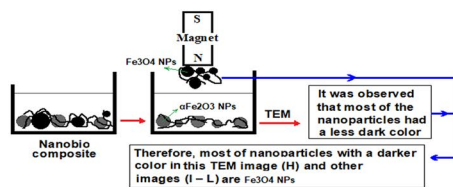
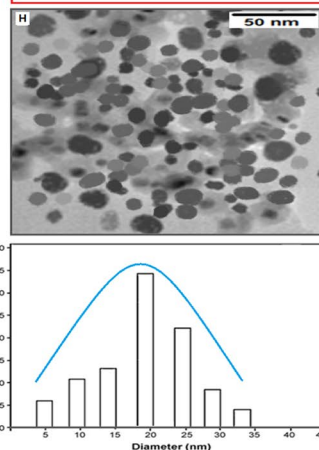
Using NCT as P1 (was synthesized separately from dye removal, removal time: 10.0 min)



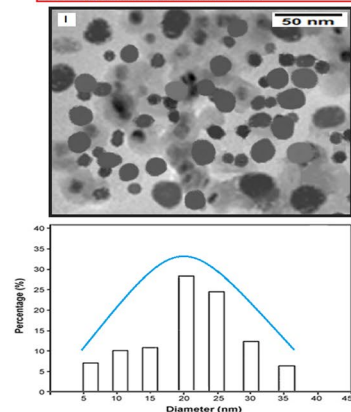
Using NCT as P2 (was synthesized simultaneously with dye removal for 10.0 min)



NPs in bare NCT with the average size less than those of NCT-BG in SAP and greater than those of NCT-BG in AA



NPs of NCT-BG in SAP for separate NCT synthesis and BG removal (by P1) by distributing the size of particles similar to them in bare NCT (without appreciably more agglomeration and or stabilization)



NPs of NCT-BG in AA for separate NCT synthesis and BG removal (by P1) by distributing the size of particles similar to them in bare NCT (without appreciably more agglomeration and or stabilization)

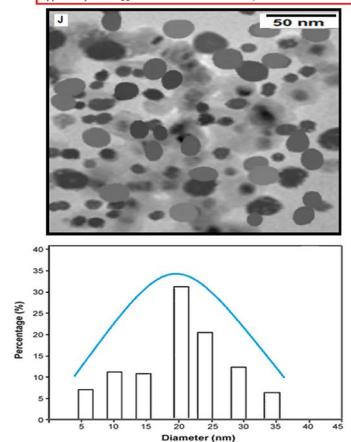
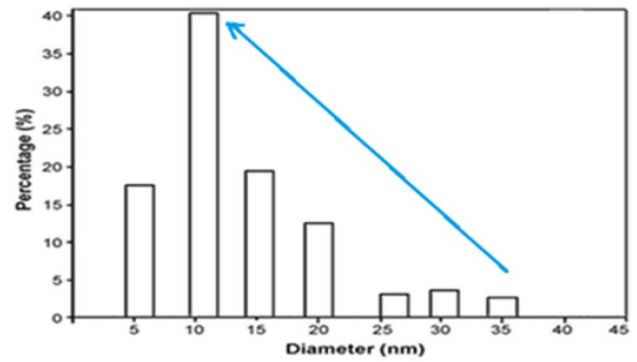
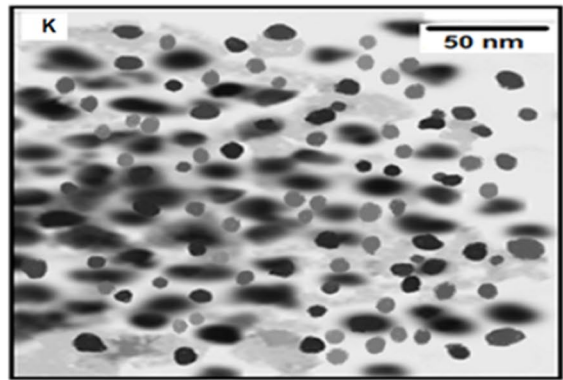
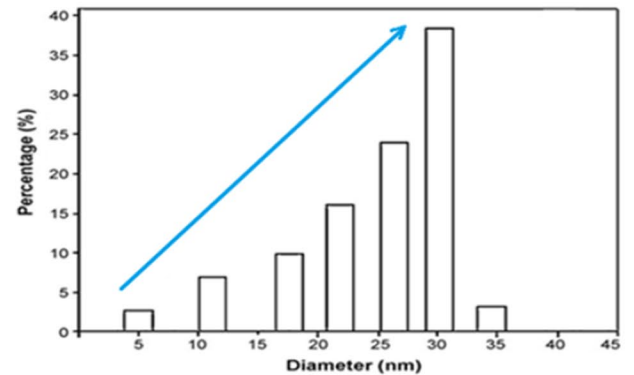
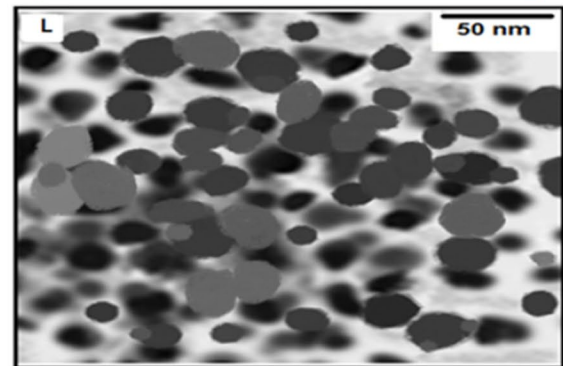


Fig. 1 (continued)

Stabilization of NPs in NCT-BG for simultaneous adsorption and photodegradation (SAP) using NCT as P2 (was synthesized simultaneously with dye removal for 10.0 min)



Agglomeration of NPs in NCT-BG for alone adsorption (AA) using NCT as P2 (was synthesized simultaneously with dye removal for 10.0 min)



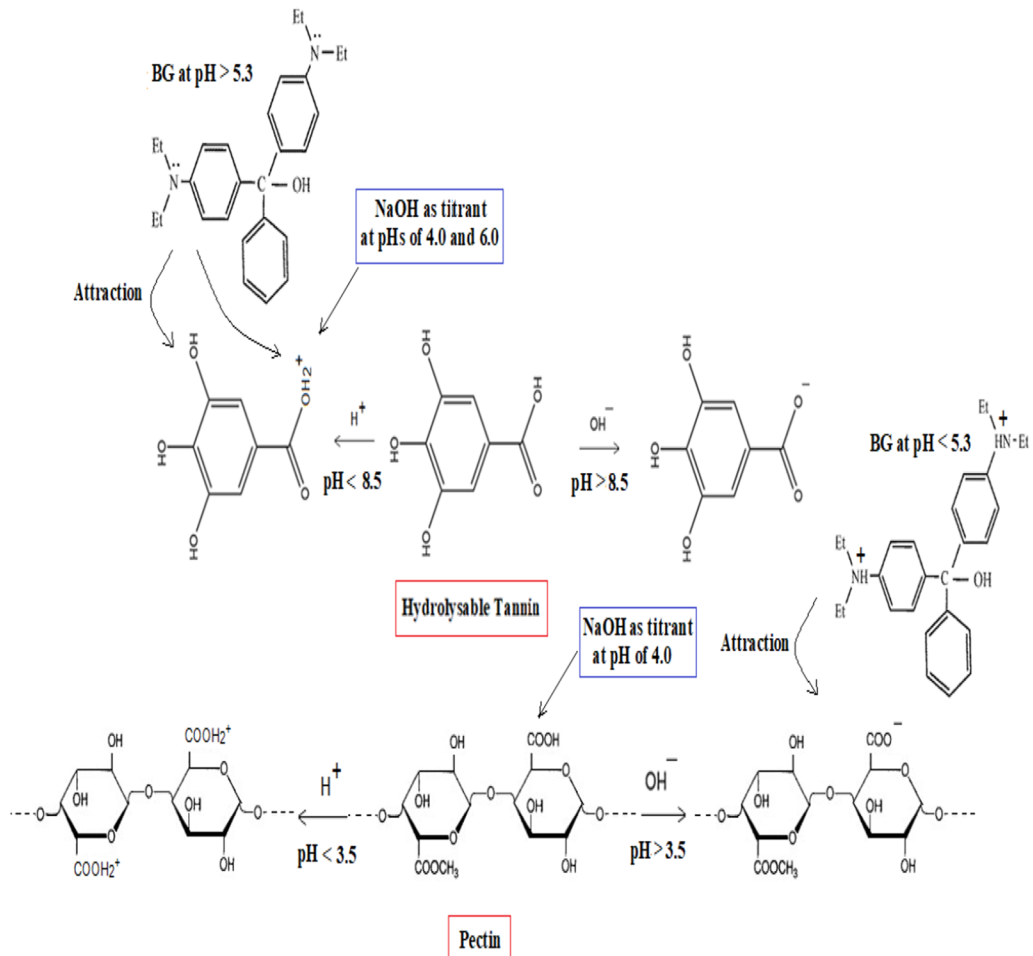
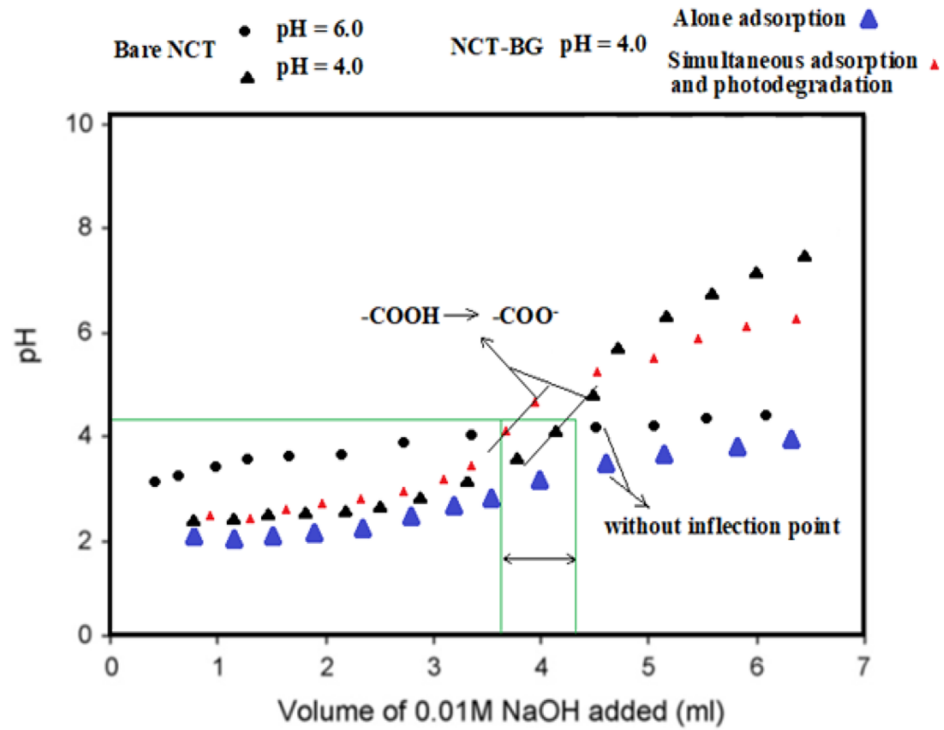


Fig. 2 Potentiometric titration curves of bare NCT treated at pHs of 4.0 and 6.0, and of NCT-BG as P1 due to alone adsorption (AA) and simultaneous adsorption and photodegradation (SAP) processes at pH of 4.0, and the scheme of pectin and hydrolyzable tannin form of nanocomposite s' LP (in α -Fe₂O₃ NPs/lemon peel (LP)/Fe₃O₄ NPs) at higher and less pHs than their PZC and interaction between the substances and BG

which is more efficient in AA. Figure 1C and E shows stabilization and agglomeration of NPs in SAP and AA, respectively, by using NCT as P2. Figure 1F shows by using P1 stabilization and agglomeration do not occur in AA, due to the maximum adsorption of dye, and the most organic substances containing C–C and C–O are present. Using P2 (Fig. 1G), due to stabilization of NPs in SAP and agglomeration of NPs in AA, respectively, more and less connection occurs between small materials resulting from dye photodegradation and or big dye molecules with nanoparticles.

Figure 1H–L shows TEM images of NCT after simultaneous adsorption and photodegradation (SAP) and alone adsorption (AA) of BG, respectively, after 30 min at pH = 10.0.

These images confirm the XPS results about the role of dye photodegradation products for the stabilization of nanoparticles compared with agglomeration done during alone adsorption.

The agglomeration of nanoparticles reduces their effective surface and performance. Usually, the presence of organic or polymer compounds as a stabilizer prevents this state.

It has been shown that the compounds obtained from the photocatalytic degradation of BG in SAP can stabilize the nanoparticles; while the BG molecules did not stabilize the nanoparticles, the aggregation of nanoparticles also occurred in AA using NCT as P2. The process of NPs stabilization in SAP causes an autocatalytic cycle. In such a way, the destruction of the dye helps to prevent the accumulation of nanoparticles to optimal performance through photocatalytic nanoparticles.

The reason for this performance difference can be due to the fact that the compounds resulting from the decomposition in SAP are smaller compared to the big dye molecules in AA, and they can better penetrate the pores of nanoparticles and prevent the interaction between them and so their agglomeration. Even on the contrary, since the BG molecules in AA are more adsorbed to the functional groups of LP in NCT, they contribute more to the accumulation of NPs compared to the bare NCT, because part of the functional groups of LP that are responsible for the NPs stabilization role were connected to BG molecules which these molecules do not have the necessary ability for NPs stabilization because on the one hand BG molecules are not the small like the photodegradation compounds that can penetrate between the nanoparticles and, on the other hand, are not wide with many active groups like the organic compounds of lemon peel.

Discussion

Pectin of LP in NCT; only effective agent to adsorb BG at pH = 4.0: Potentiometric titration to obtain contribution of pectin in simultaneous adsorption and photodegradation (SAP)

Potentiometric titration curves show the one inflection points at approximately pH 4.3–4.5, which corresponds to pKa values of carboxyl–carboxylate equilibrium point. Pectin as one of the components of lemon peel has –COOH/–COOCH₃ groups. Also, one of the main tannin forms as a polyphenol is the hydrolyzable structure which has –COOH functional group. So they can neutralize alkaline titrant. But hydrolyzable tannin having the same charge with BG charge at pH = 4.0 does not have appreciable adsorption; in addition, it has its group as –COOH₂⁺ and so does not show the inflection point of carboxyl–carboxylate equilibrium.

Pectin has the negative surface charge like BG, at pHs of 6.0 and 10.0. Therefore, due to the repulsion between dye and pectin, BG adsorption on pectin of NCT can be ignored at these pHs. For this reason, the amount of adsorption is evaluated using potentiometric titration between BG and NCT treated (NCT-BG) as P1 at pH = 4.0; due to the same electrical charges (as positive) of BG and all effective components of NCT except pectin, adsorption between them is insignificant. In the other words, the only BG adsorbing agent by NCT at pH = 4.0 is pectin of LP in NCT.

As can be seen from Fig. 2, for both the bare NCT and NCT-BG states that were treated in pH = 4.0, the inflection point was observed at pH of 4.5–4 in potentiometric titration, which indicates the conversion of –COOH to –COO[–] related to pectin. Because as it can be seen, it is only pectin that is in acid form around pH = 3.5, and therefore that part of it that is not converted to –COO[–] in pHs of about 3.5 (pH = 4.0) is converted to –COONa in the presence of the added NaOH as the titrant.

The difference between the mentioned two curves is in the amount of titrant used to neutralize the –COOH of pectin, which is about 0.6 ml less in the case of the NCT-BG due to the simultaneous adsorption and photodegradation compared with bare NCT, because the BG⁺ that remains in molecular form and does not photodegraded can be adsorbed by –COO[–] of pectin (at pH = 4; 3.5 < pH < 5.3), and therefore, it is possible to perform fewer conversions from –COOH to –COO[–] which causes less NaOH consumption.

In the simultaneous adsorption and photodegradation process, [COOH] = $[(V_{eq1}(\text{NaOH}) \times C_{\text{NaOH}}) / m] = [(3.7 \times 0.01) / 3.0] = 0.012 \text{ mmol/g}$

$$= [(3.7 \times 0.01) / 3.0] = 0.012 \text{ mmol/g.}$$

In the bare NCT, [COOH] = $[V_{eq2}(\text{NaOH}) \times C_{\text{NaOH}}] / m$
[COOH] = $[V_{eq2}(\text{NaOH}) \times C_{\text{NaOH}}] / m = [(4.3 \times 0.01) / 3.0] = 0.014 \text{ mmol/g.}$

It is equal to the value of $-\text{COOH}$ groups of pectin in NCT which does not interfere for the dye adsorption in the simultaneous adsorption and photodegradation process at $\text{pH}=4$.

So $\Delta [\text{COOH}] = [\Delta V_{\text{eq}(\text{NaOH})} \times C_{\text{NaOH}}] / m = [(0.6 \times 0.01) / 3.0] = 0.002 \text{ mmol/g}$.

It is equal to the value of $-\text{COOH}$ groups which interferes for the adsorption of dye in the simultaneous adsorption and photodegradation process at $\text{pH}=4.0$.

If, ideally, each BG molecule with its positive electric charge is attached to two pectin carboxylate groups from one or two pectin chains from its two sides (through two groups

$-\text{NH}(\text{Et})_2$), then each BG molecule with two moles carboxylate related. So 0.002 mmol of the mentioned carboxyl is connected to 0.001 mmol or 0.47 mg BG for each gram NCT at $\text{pH}=4.0$.

The difference between the primary BG used in total and this amount (0.47 mg) is equal to about the amount of BG that is photodegraded and or adsorbed by other adsorbents of NCT.

Initial BG mass/ NCT = $10.0 \text{ ppm} \times 10.0 \text{ ml} = 0.10 \text{ mg} / 0.05 \text{ g} = 2.00 \text{ mg/g}$.

Total BG removed at pH of 4.0 in simultaneous adsorption and photodegradation = $93.3\% \times 10.0 \text{ ppm} = 9.3 \text{ ppm} \times 10.0 \text{ ml} = 0.093 \text{ mg}$ total BG removed/0.05 g = 1.86 mg/g.

Therefore, the mass of BG removed by other ways includes adsorption by other matters and photodegradation at pH of 4.0 = $1.86 - (0.47 \text{ mg/g removed by adsorption on } -\text{COO}^- \text{ of pectin}) = 1.39 \text{ mg/g}$. Because, as mentioned, the contribution of BG adsorption by other components of NCT in $\text{pH}=4.0$ due to the same electric charge is insignificant, 1.39 mg/g is about the contribution of photodegradation in the simultaneous process.

On the other hand, for the bare NCT treated at $\text{pH}=6.0$ and NCT-BG due to alone adsorption at $\text{pH}=4.0$, no inflection point can be seen in 4.5–4.5 during titration, which indicates the absence of significant presence of $-\text{COOH}$ in both pectin and tannin in these samples. According to Fig. 2, there is no free $-\text{COOH}$ in $\text{pH}=6$, and although there is a possibility of the presence of $-\text{COOH}$ groups in the bare NCT at $\text{pH}=4.0$, for NCT-BG after alone adsorption, the maximum value of BG^+ is adsorbed to $-\text{COO}^-$ of pectin in NCT, and it does not allow the NaOH to convert $-\text{COOH}$ to salt $-\text{COO}^-$.

These results show that almost a significant amount of free $-\text{COOH}$ groups does not remain in NCT-BG at $\text{pH}=4.0$ in alone adsorption (AA), and in other words, all of them participated in BG absorption. Also, according to the investigations carried out on nanoparticles that show the amount of adsorbed dye (by PPA method in Sec. 3.5), it is clear that any BG that is not adsorbed by pectin of LP is only adsorbed

by nanoparticles and no dye is absorbed by other organic substances of LP in NCT at pH 4.0 in AA.

Determination of contribution of effective alcohols, Cellulose and Hydrolyzable tannin of LP in NCT as P1 and P2 to adsorb BG at $\text{pH}=6.0$ using AMI method and confirmation of results by PPA method

Acetic anhydride (A) can react with $-\text{OH}$ of bioorganic matter in the presence of and microwave irradiation (M) and iodine (I) (Zhang et al. 2019). In this study, the AMI method is named.

Hydrolyzable tannin, cellulose, and linalool, borneol and fenchol, alcohols of LBF (TCA) are the main organic agents in lemon peel of NCT which have $-\text{OH}$ as the similar functional groups for the adsorption of BG. Other alcohols of LP have very small amounts and do not have a significant effect on dye adsorption.

Therefore in this study, the same method was chosen to measure the hydroxyl of them and finally to determine BG adsorbed by these organic agents.

If the mass balance of the adsorbed dye is established in the mentioned method, which is specific to the molecules with $-\text{OH}$ groups in LP of NCT, then only the molecules of LBF, cellulose and hydrolyzable tannin can be considered as the only dye adsorption factors in $\text{pH}=6.0$ and that the same situation will be observed and proven. pK_a of linalool, borneol and fenchol (effective alcohols of LBF for BG removal) is 14.5–15.3, so it has the positive charge due to their $-\text{OH}_2^+$ groups at pH s of 4.0, 6.0 and 10.0, similar to cellulose. Because BG is positive at pH of 4.0, so its adsorption is negligible by TCA, so that AMI method in this section and PAA method by evaluating consumed titrant showed that the adsorption of BG by TCA and NPs was negligible, respectively, at $\text{pH}=4.0$. It can be expected due to the same electrical charge of BG and TCA components and nanoparticles (Table 1). Therefore, the only main BG adsorption agent in this pH was pectin of LP in NCT.

But at pH s of 6.0 and 10.0 that the dye is as BG^- due to its free pair electrons, its adsorption can be happened by cellulose and alcohols of LBF with their positive charges. Therefore to evaluate the ability of cellulose and LBF to adsorb dye, NCT-BG treated at pH s of 6.0 was selected to study by anhydride acetic test.

As can be seen from Fig. 3, for the samples of S1, S2 and S3, 10 ml of acetic anhydride 1.0 mM (10.0 mmol) is used and shake 1.0 h, separately. Then the mixture was treated with iodine 15mol% under microwave irradiation with power 300 W for 20 min. After separation mass, the remained anhydride is washed by distilled water. Then, it was neutralized by NaOH 0.01 M as titrant to determine the unreacted acetic anhydride.

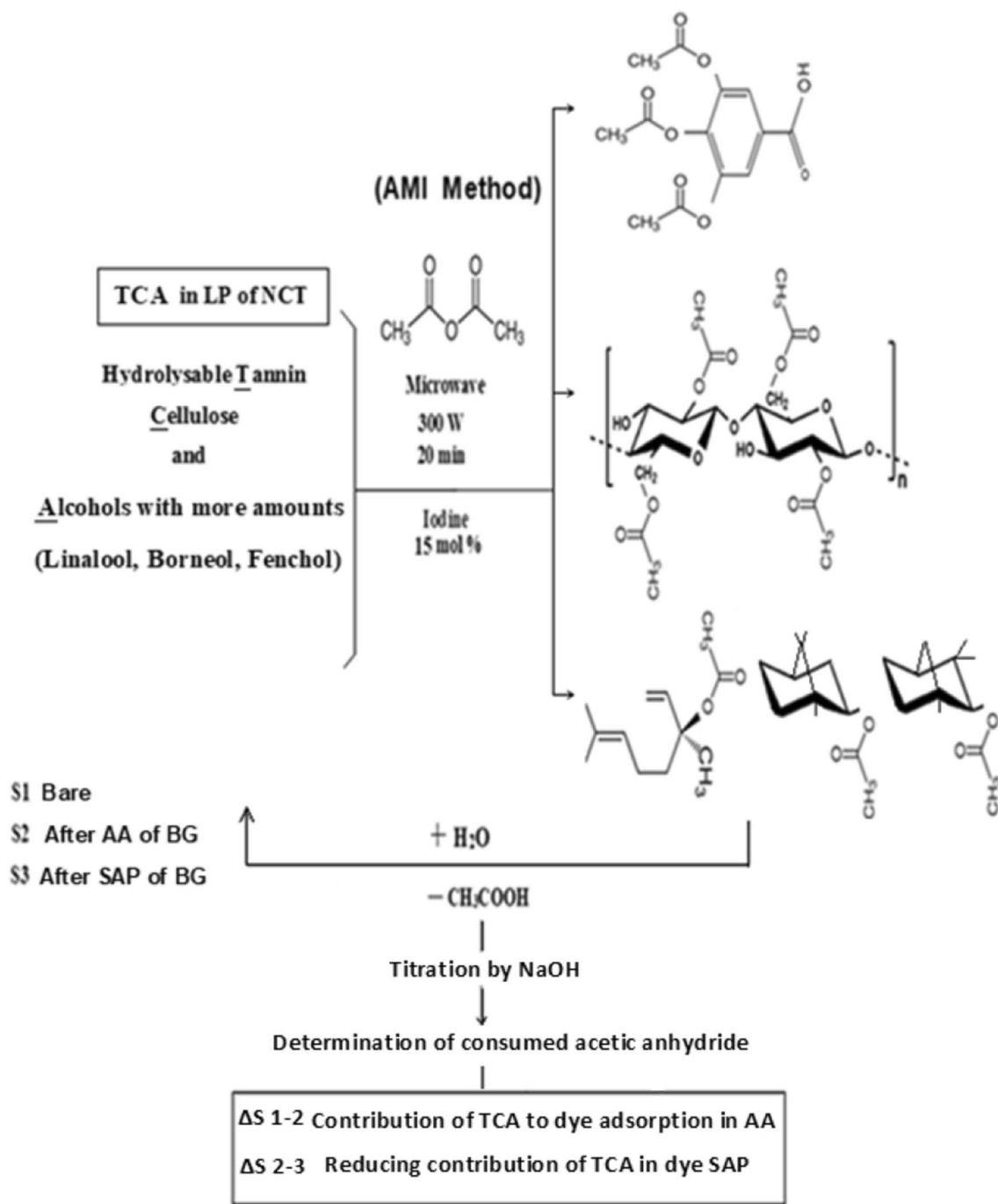


Fig. 3 Reaction between TCA of nanocomposite s' LP (in α -Fe₂O₃ NPs/lemon peel (LP)/Fe₃O₄ NPs) as P1 and P2 with acetic anhydride in the presence of iodine under 300W microwave

$(\text{CH}_3\text{CO})_2\text{O}$ (free) is not reacted + $\text{H}_2\text{O} \rightarrow 2 \text{CH}_3\text{COOH}$.

$\text{NaOH} + \text{CH}_3\text{COOH} \rightarrow \text{CH}_3\text{COONa} + \text{H}_2\text{O}$.

$1 \text{mmol NaOH} \equiv 0.5 \text{mmol}(\text{CH}_3\text{CO})_2\text{O}$ (free)

On the other hand,

$S = [\text{mmol consumed } (\text{CH}_3\text{CO})_2\text{O}]$

$= [A \text{ mmol initial } (\text{CH}_3\text{CO})_2\text{O}] - [B \text{ mmol free } (\text{CH}_3\text{CO})_2\text{O}]$.

$= [C \text{ mmol connected } \text{CH}_3\text{CO}-] + [C \text{ mmol free } \text{CH}_3\text{COOH}]$,

that $B = (C/2)$.

Because any $-OH$ group in organic matters can react with $(CH_3CO)_2O$, it can naturally participate in BG adsorption at $pH=6.0$, so about $1\text{ mmol } (CH_3CO^-) \equiv 1\text{ mmol BG}$, so.

$1\text{ mmol NaOH} \equiv 0.5\text{ mmol } (CH_3CO^-) \equiv 0.5\text{ mmol BG}$

The BG adsorption can be done at $pH=6.0$ by organic matters (alcohols of LBF, cellulose and hydrolyzable tannin) except pectin which has the same surface charge with BG at pH of 6.0.

In order to determine the contribution of $(CH_3CO)_2O$ absorption by Fe_3O_4 NPs and $\alpha-Fe_2O_3$ NPs (both together and separately) and the contribution of BG absorption by only the organic matters in LP of NCT as P1 and P2, the same amount of each nanoparticles synthesized in NCT was synthesized separately (without LP) and placed in contact with the same amounts of $(CH_3CO)_2O$ under the same conditions. The results for NCT as P1 showed that the alone nanoparticles ($\alpha-Fe_2O_3$ and Fe_3O_4) can adsorb $0.47\text{ mg BG}/0.23\text{ g NPs}$ which is because the amount of nanoparticles used in each g NCT is equal to 0.23 g (0.23 g NPs/g NCT); therefore, the BG adsorption by NPs of NCT is 0.47 mg BG/g NCT . 0.49 mg/g was obtained due to the evaluation of the BG adsorption by nanoparticles in alone adsorption by PPA method which shows a good closeness of the data.

This experiment was also done for the simultaneous adsorption and photodegradation (SAP) to evaluate BG adsorption capacity by NPs of NCT which was obtained 0.12 mg/g . So 0.36 mg/g ($0.48-0.12$) was photodegraded, obtaining 0.38 mg/g in the study of PPA method in Sect. 3.2.7 which is a good confirmation.

Therefore, the difference between the NaOH consumed due to the adsorption of $(CH_3CO)_2O$ and so BG by NCT as P1 from NaOH consumed that of alone nanoparticles can be evaluated as the ability of BG adsorption by only organic agents of NCT as presented below:

$(S1-S2) \equiv 0.094\text{ mmol NaOH}/20\text{ g}$ for NCT-BG was obtained in alone adsorption at pH of $6.0=0.047\text{ mmol BG}/20\text{ g NCT}$ (1.11 mg/g). 1.12 mg/g was obtained due to the evaluation of the BG adsorption by organic matters in PPA method which shows a good closeness of the data.

$(S2-S3) \equiv$ (less adsorbed dye in the simultaneous process compared to alone adsorption process which is equal to the photodegraded dye) $\equiv 0.030\text{ mmol NaOH}/20\text{ g}$ in simultaneous adsorption and photodegradation process at pH of $6.0 \equiv 0.015\text{ mmol BG}/20\text{ g NCT}$ (0.36 mg/g).

It has very little difference from 0.36 mg/g (obtained from the test mentioned above which was done in the case of alone nanoparticles). 0.38 mg/g is obtained in PPA test as the BG photodegraded value in simultaneous process shows a good closeness of the data.

While using NCT as P2, NPs stabilization by components resulting from photodegradation and its effect on the adsorption of more dye, and also NPs agglomeration during AA

process and its effect on decreasing the adsorption of dye were investigated.

The NPs that had been stabilized in the SAP strongly adsorbed the dye, and on the contrary, during the AA process, the nanoparticles that had agglomerated and accumulated in the AA strongly reduced adsorbing the dye. The obtained products were used to determine the adsorbed BG by TCA according to the mentioned AMI method. The quantities obtained using P2 in a similar way to P1 are shown in Fig. 4. As can be seen from Fig. 4, with the increase and decrease in the share of nanoparticles in dye adsorption, the share of organic substances of LP in NCT in dye adsorption decreases and increases, respectively.

Synthesis of Fe_3O_4 NPs-PPA and $\alpha-Fe_2O_3$ NPs-PPA to determine the contribution of $\alpha-Fe_2O_3$ NPs and Fe_3O_4 NPs of NCT as P1 and P2 to adsorb BG at $pH=6.0$ and confirmation of results by AMI method

$Fe-O-O-H$ and $Fe-O-H$ structures in the $\alpha-Fe_2O_3$ NPs surface and $Fe-O-H$ structure in the Fe_3O_4 NPs surface as well as more hydroxyl groups are observed, promoting the adsorption performance since the process is mainly influenced by complexation via coordination bonds (Liu et al. 2020) (Fig. 5(A1–3) and B). As can be seen from Fig. 5A2 and 3, each 3-phosphonopropionic acid (PPA) molecule has two $-OH$ groups which can attach to the hydroxyl groups on the surfaces (Wang et al. 2016) such as of Fe_3O_4 NPs surface through the phosphonate groups to form strong covalent bonds (Cedrowska et al. 2020).

Because $\alpha-Fe_2O_3$ NPs also have surface $-OH$ groups, in this study, the mentioned method is used to connect PPA with $\alpha-Fe_2O_3$ NPs, in addition to Fe_3O_4 NPs. 10.0 mL of 0.1 M NaOH was mixed with 30 mL of 20.0 mg/ml (3.89 mmol) of 3-phosphonopropionic acid (PPA) 3.0 min and then was added to 1.00 g NCT as P1 and P2, separately. The suspension was dispersed for 20 min in an ultrasonic bath, and the treated NCT was separated from unreacted PPA by filter paper and washed a few times with deionized water. At last, the unreacted PPA was titrated by NaOH (0.010 M) to obtain the used PPA and finally to determine $-OH$ consumed to adsorb BG.

It was found that $-OH$ groups of organic agents in LP have no significant connection with PPA according to the used titrant (NaOH) and the comparison between the initial and residual PPA.

This state can be due to the low contact surface of components with hydroxyl and high crowding of organic tissue (compared to nanoparticles) in LP and also low penetration of PPA into this dense tissue.

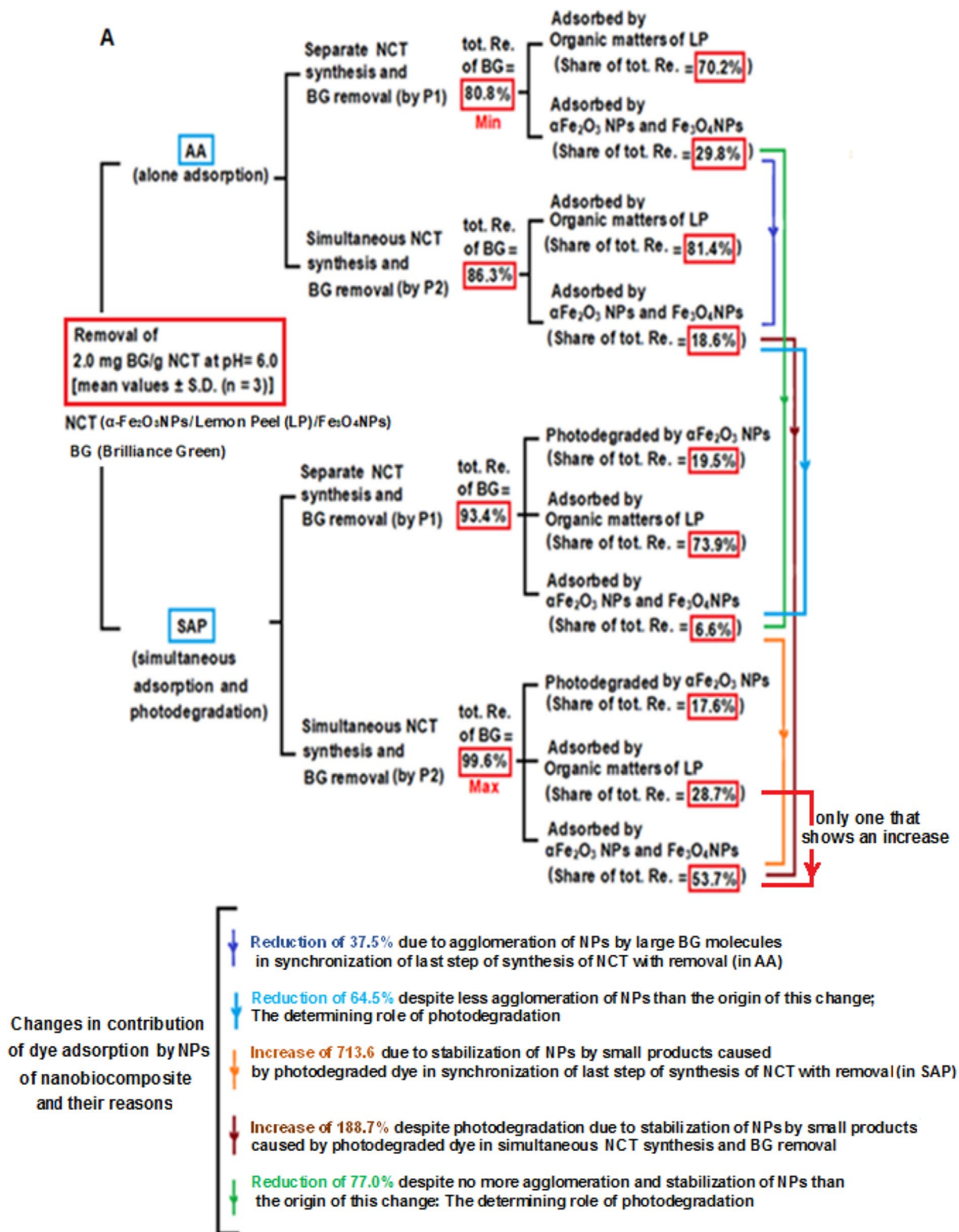


Fig. 4 A and B The mass balances and quantitative contribution of BG removed by different substances of NCT during alone adsorption (AA) and the simultaneous adsorption and photodegradation (SAP) processes in batch unit at pHs of 4.0 and 6.0, and effect of separate

and simultaneous synthesis of NCT with BG removal process (using P1 and P2) on changes of contribution of BG adsorption and photodegradation by different substances of NCT with the mean values ± S.D. (n = 3)

B The effective components in NCT
(both in terms of quantity and functional groups) for BG removal
AA: Alone adsorption SAP: Simultaneous adsorption and photodegradation

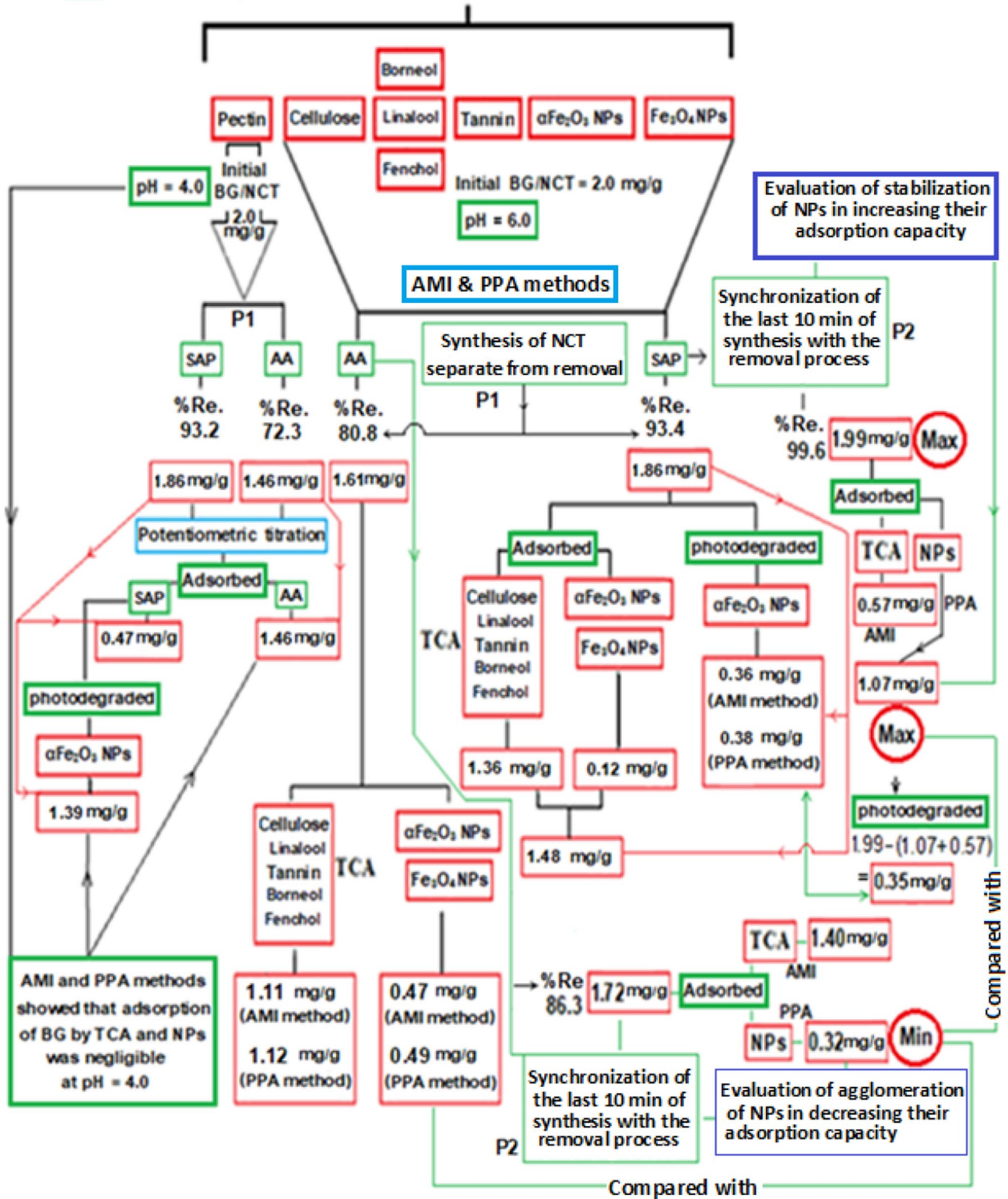


Fig. 4 (continued)

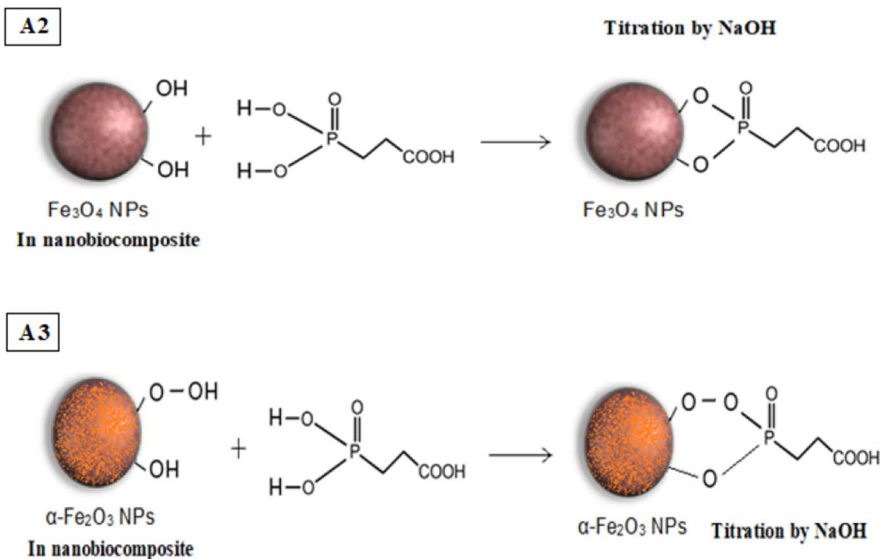
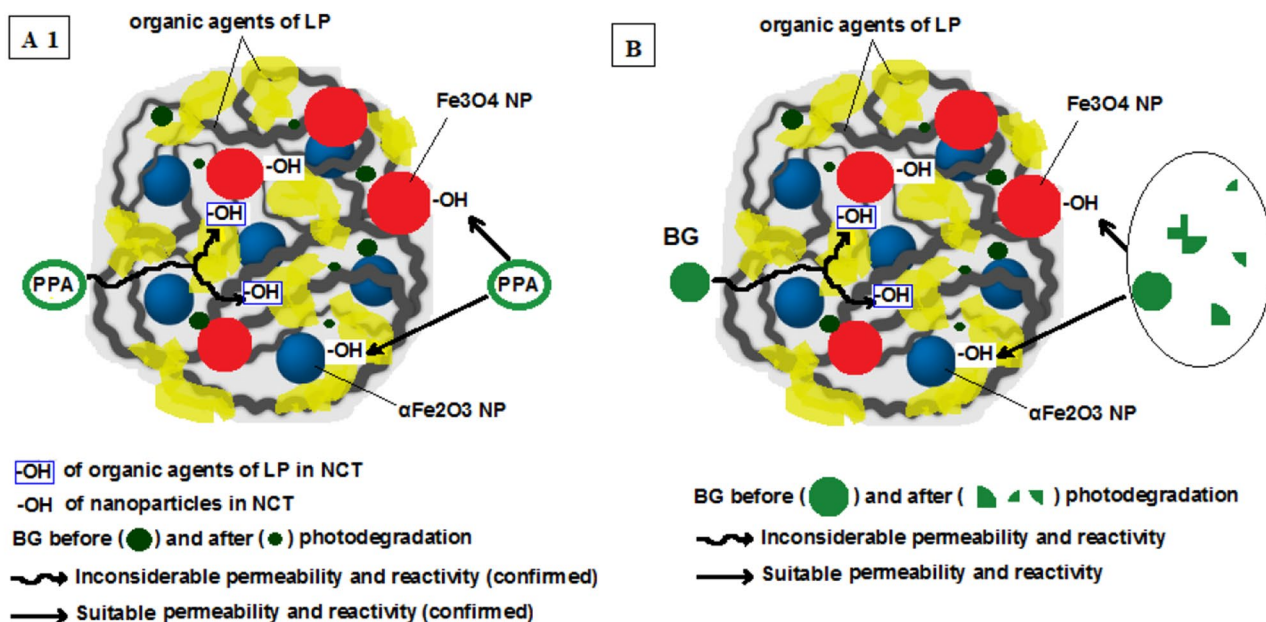


Fig. 5 Reaction between nanoparticles of NCT ($\alpha\text{-Fe}_2\text{O}_3$ NPs/ lemon peel (LP)/ Fe_3O_4 NPs in optimum form) and PPA (A1, A2 and A3), and in a similar order and reason about permeability (in A1), between

nanoparticles of NCT and BG before (in AA) and after (in SAP) photodegradation (B)

Therefore, all PPA consumed in contact with NCT can be considered due to connection with NPs of NCT.

Also, to determine the amount of reaction between organic agents of LP containing -OH (such as alcohols and cellulose) and PPA and the amount of titrant used for unreacted PPA (after reaction between NPs of NCT and PPA), under the same conditions, the same investigation was carried out, separately for NCT (that contains both LP and nanoparticles) and alone NPs. The difference between the amounts of titrant used for these samples was used to

determine the share of PPA that reacts with the LP and so with NPs of NCT.

Fe_3O_4 NPs and $\alpha\text{-Fe}_2\text{O}_3$ NPs have the positive charge due to their $-\text{OH}_2^+$ groups at pH of 6.0 and BG has the negative charge due to its free pair electrons, so adsorption can be happened between them. Therefore to evaluate the ability of Fe_3O_4 NPs and $\alpha\text{-Fe}_2\text{O}_3$ NPs to adsorb BG by NCT, NCT-BG treated at pH of 6.0 was selected to study by 3-phosphonopropionic acid test, similar to the study of interaction between cellulose and LBF alcohols with anhydride acetic.

The difference between PPA used and the remaining PPA in the solution after separating the solid matter containing NCT (which determined due to titration by NaOH 0.01M) shows the amount of PPA reacted with nanoparticles in NCT. On the other hand, if nanoparticles by their $-\text{OH}_2^+$ groups adsorb BG^- at $\text{pH}=6.0$, the available positions of nanoparticles to react with PAA are reduced, so that any increase in the amount of NaOH consumed indicates a decrease in the PAA attached to nanoparticles due to the binding of dye molecules.

$1 \text{ mmol NaOH} \equiv 1 \text{ mmol PPA} \equiv 2 \text{ mmol } -\text{OH} \text{ (of NPs)} \equiv 1 \text{ mmol BG}^-$ (at $\text{pH}=6.0$, which is a share of $-\text{OH}$ groups of NPs as $-\text{OH}_2^+$ according to Table 1A).

The results showed that the used mmol of NaOH (0.010 M) for neutralization of free PPA was 0.061 mmol (6.1 ml); for the bare NCT, it was 0.081 mmol (8.1 ml); for NCT-BG as P1 due to the alone adsorption, 0.065 mmol (6.5 ml) NaOH was obtained for NCT-BG as P1 due to the simultaneous adsorption and photodegradation process. As can be seen, the consumption of NaOH mmol or actually the unbound PPA in the alone adsorption process is more than the other two cases, which indicates the maximum occupation of functional groups on the surface of nanoparticles by the dye.

As expected, the amount of NaOH mmol consumed in the case of the simultaneous process is less than the amount in the case of the alone absorption process, which is due to the destruction of part of the dye molecules and the impossibility of attaching them to the nanoparticles. Instead, it provides more possibility for PPA to bind nanoparticles. As a result, less free acid remains, and NaOH mmol consumption is reduced. Therefore, 0.020 (0.081–0.061) mmol $\text{BG}/20.0 \text{ g NCT}$ as P1 or 0.49 mg/g was adsorbed on Fe_3O_4 NPs and $\alpha\text{-Fe}_2\text{O}_3$ NPs in the alone adsorption (AA) process at $\text{pH}=6.0$, due to reduction in the share of adsorption of organic matter. Also, 0.016 (0.081–0.065) mmol $\text{BG}/20.0 \text{ g NCT}$ as P1 or 0.38 mg/g ($20.4\% = 0.38/1.86$) did not adsorb on Fe_3O_4 NPs and $\alpha\text{-Fe}_2\text{O}_3$ NPs in the simultaneous adsorption and photodegradation (SAP) process and it is photodegraded at $\text{pH}=6.0$.

In other words, 80.8% of BG removal at $\text{pH}=6.0$ (for 10.0 ml of 10.0 ppm/ 0.05 g or 2.0 mg/g) equal to 1.61 mg/g as the BG removal value in alone adsorption (AA) process by NCT as P1, 0.49 mg/g ($30.4\% = 0.49/1.61$) is removed due to the adsorption on Fe_3O_4 NPs and $\alpha\text{-Fe}_2\text{O}_3$ NPs, and so about 1.12 mg/g (1.61 -0.49) or 69.6% BG^- is removed (was confirmed by $(\text{CH}_3\text{CO})_2\text{O}$ test in Sec. 3.5 due to adsorption on other agents in NCT including cellulose, alcohols of LBF and tannin (BG^- adsorption on pectin is insignificant due to its negative charge at $\text{pH}=6.0$).

On the other hand, 93.4% of BG was removed at $\text{pH}=6.0$ (for 10.0 ml of 10.0 ppm/ 0.05 g or 2.0 mg/g) equal to 1.86 mg/g in the simultaneous adsorption and photodegradation (SAP) process by NCT as P1, and 1.48 mg/g (1.86–0.38) or 79.5% (1.48/1.86) BG was removed due to adsorption on Fe_3O_4 NPs, $\alpha\text{-Fe}_2\text{O}_3$ NPs and cellulose, LBT and tannin. Therefore about 0.38 mg/g ($0.38/1.86 = 20.4\%$) was photodegraded in the simultaneous adsorption and photodegradation process. 0.36 mg/g was obtained by $(\text{CH}_3\text{CO})_2\text{O}$ test (AMI method) that the closeness of the data is a suitable confirmation of the investigation.

Since the amount of dye adsorption by alone nanoparticles was obtained 0.12 mg/g; therefore, 1.36 mg $\text{BG}/\text{g NCT}$ as P1 (1.48–0.12) was adsorbed by cellulose, LBF and tannin (without nanoparticles), in the simultaneous adsorption and photodegradation process at $\text{pH}=6.0$.

To investigate NPs stabilization by components resulting from photodegradation and its effect on the adsorption of more dye and NPs agglomeration during AA process and its effect on decreasing the adsorption of dye, after SAP and AA processes using NCT as P2, it was done according to the mentioned ways for P1. The quantities obtained for PPA method using P2 are shown in Fig. 4. The obtained products were used to determine the adsorbed BG by NPs according to the mentioned PPA method. As can be seen from Fig. 4, with the increase and decrease in the share of NPs in dye adsorption, the share of organic substances of LP in NCT in dye adsorption decreases and increases, respectively, which was confirmed by AMI method (Sect. 3.4).

Based on these findings, it can be concluded that in AA if the NCT synthesis is done simultaneously with removal process (as P1), due to the decrease in the efficiency of NPs and their agglomeration, less nanoparticles can be consumed because the LP of NCT itself helps to more adsorption. In SAP, simultaneous synthesis of NCT with dye removal (P2) increases the ability of NPs due to their stabilization, and by increasing the amount of nanoparticles used, more adsorption and removal efficiency can be achieved.

Also, according to these mass balances other molecular components of LP in NCT are not effectively involved in dye removal.

Kinetic and thermodynamic of BG removal in SAP and AA by NCT as P1 and P2

For investigating the photocatalyst degradation ratio of BG dye in SAP by NCT as P1 and P2, first- and second-order kinetics is used in optimum situation. These models are given by the following equations:

Table 3 Kinetic constants of BG removal by NCT as P1 and P2 in SAP and AA processes

Method and kind of NCT	K1 (1/min)	R ²	K2 (L/mg.min)	R ²
AA by P1	0.152	0.723	0.823	0.992
AA by P2	0.172	0.786	0.923	0.998
SAP by P1	0.179	0.993	0.641	0.734
SAP by P2	0.253	0.998	0.762	0.812

$$\text{Ln}\left(\frac{C_0}{C}\right) = k_1t \tag{1}$$

Equation (1) is the first-order kinetic where the terms C₀ (ppm), C_e (ppm) and k₁(1/min) sequential are initial dye concentration, the remaining concentration of dye after the UV-C light effect and the first-order rate constant. A plot of Ln(C₀/C) versus time represents a straight line, the slope of which upon liner regression equals the first-order rate constant (K₁), which was obtained 0.179 1/min with R²=0.993 in the room temperature.

The second-order kinetic model is shown in Eq. (2):

$$\frac{1}{C_e} - \frac{1}{C_0} = k_2t \tag{2}$$

The terms C₀ (ppm), C_e (ppm) and k₂(L/mg.min) sequential are initial dye concentration, the remaining concentration of dye after the UV light effect and the second-order rate constant. A plot of 1/C_e - 1/C₀ versus time represents a straight line, the slope of which upon linear regression equals the second-order rate constant (K₂) which was obtained 0.641 l/mg.min with R²=0.734 in the room temperature. So it follows the first-order kinetic model.

In alone adsorption (AA) process of BG by NCT, pseudo-first-order [log(q_e - q_t) = Log(q_e) - (k₁/2.3)t] and pseudo-second-order [t/q_t = 1/(K₂q_e²) + t/q_e] kinetic models were used and q_e=(C₀-C_e)/m and q_t are the adsorption capacity (mg/g) at equilibrium and time of t, respectively. q_e(exp) and q_e(cal) were obtained 1.992 and 0.350 mg/g from pseudo-first-order with R²=0.821, while obtained 1.992 and 1.980 mg/g from

pseudo-second-order model with R²=0.992. So it follows the pseudo-second-order kinetic model. Table 3 shows that AA in both using NCT as P1 and P2 is done according to the second order, while SAP in both using NCT as P1 and P2 is done according to the first-order kinetic model. On the other hand, the kinetic constants using NCT as P2 are higher in SAP due to their NPs stabilization.

The Eyring–Polanyi equation can describe the variance of the rate of a chemical process with temperature (Zamani et al. 2018). The linear form of this Eq. (3) is as follows:

$$\text{Ln}\left(\frac{k_1}{T}\right) = -\left(\frac{\Delta H}{R}\right)\frac{1}{T} + \text{Ln}\frac{K_B}{h} + \frac{\Delta S}{R} \tag{3}$$

$$\text{Ln}[(k.h)/(K_B.T)] = -(\Delta H/R)1/T + \Delta S/R \tag{4}$$

where k is the rate constant of first-order kinetic (1/sec), K_B = 1.38066 × 10⁻²³(J/K) is the Boltzmann constant, R = 8.314(J/mol.K) is the universal gas constant, h = 6.626 × 10⁻³⁴(J.sec) is the Planck constant, and ΔH⁰(J/mol) and ΔS⁰(J/mol.K) are sequential changes of enthalpy and entropy. The amounts of ΔH⁰ and ΔS⁰ were determined from the slope and the intercept of the linear plot of Ln(K₁/T) vs.1/T. The change of Gibbs free energy (ΔG⁰) can be acquired via the Van't Hoff equation. The final concentration of BG dye (C₀ = 10mg/L) was calculated at pH = 7 and different temperatures.

It shows that the processes of SAP (using both P1 and P2) are exothermic (ΔH⁰ < 0) and the Gibbs free energy shows the spontaneous process (ΔG⁰ > 0) with the decrease in disorder (ΔS⁰ < 0), unlike those of AA (Table 4).

The results of the two methods clearly show that high endothermicity in the alone adsorption causes it to be non-spontaneous, while in the simultaneous method, the presence of the photodegradation strongly changes the heat exchange and it changes to exothermicity, and finally the simultaneous process becomes spontaneous. In the meantime, the thermodynamic situation for the spontaneous dye removal process becomes more favorable when the stability of nanoparticles occurs in the simultaneous synthesis and removal process (using P2 in SAP). Instead, the situation is more difficult for when the accumulation and agglomeration occur in separate synthesis and removal process (using P1 in AA).

Table 4 Thermodynamic results from the Eyring–Polanyi equation for BG removal by NCT as P1 and P2 in SAP and AA processes

Method and kind of NCT	R ²	ΔH ⁰ (KJ/mol)	ΔS ⁰ (KJ/mol.K)	ΔG ⁰ (KJ/mol) (293 K)	ΔG ⁰ (KJ/mol) (313 K)	ΔG ⁰ (KJ/mol) (333 K)
SAP by P1	0.933	- 1.659	- 0.265	75.985	81.285	86.585
AA by P1	0.992	+ 10.936	+ 0.073	- 9.694	- 10.650	- 12.126
SAP by P2	0.998	- 3.452	- 0.316	89.121	94.214	103.521
AA by P2	0.988	+ 14.356	+ 0.089	- 11.963	- 14.254	- 16.278

Table 5 The factors and results for the alone adsorption process using NCT as P1

Run	Factor 1	Factor 2	Factor 3	Factor 4	Factor 5	Response 1	
	A:pH	B:time min	C:Dose g/L	D:C ₀ ppm	E:T °C	Re	
						%	
					Actual value		Predicted value
1	4	10	5	10	20	72.3425	72.11
2	6	10	5	10	20	80.7912	80.45
3	7	10	5	10	20	83.8639	83.55
4	8	10	5	10	20	93.0494	92.38
5	10	10	5	10	20	92.3414	91.89
6	7	5	5	10	20	96.2158	96.38
7	7	10	5	10	20	94.7239	94.55
8	7	30	5	10	20	94.3039	94.56
9	7	60	5	10	20	93.4224	93.46
10	7	10	1	10	20	89.3253	88.79
11	7	10	3	10	20	94.6636	95.30
12	7	10	5	10	20	93.7239	93.55
13	7	10	10	10	20	94.8844	94.71
14	7	10	20	10	20	94.7904	94.78
15	7	10	5	5	20	90.0719	90.27
16	7	10	5	10	20	83.8639	83.55
17	7	10	5	15	20	88.1276	88.91
18	7	10	5	20	20	82.6914	82.33
19	7	10	5	40	20	80.2145	80.02
20	7	10	5	10	7	94.4919	94.55
21	7	10	5	10	20	95.7239	95.55
22	7	10	5	10	40	96.0719	96.55

Statistical modeling for simultaneous adsorption and photodegradation, and alone adsorption

A response surface methodology (RSM)

In Table 5 (for alone adsorption process) and Table 6 (for simultaneous adsorption and degradation process) for NCT as P1, it can be noticed about the factors and results that is fitted by the historical section of Design Expert 11.0. The removal efficiency percent (%Re) of BG dye was considered by ANOVA as a statistical idea, for investigating the effect of the subjected factors and their interaction on dye adsorption and photodegradation by NCT (Tables 7 and 8). By considering the F-value and p-value (that must be significant) and the value of lack of fit (as a non-significant data), it can be investigated that the chosen equation for the studied process can be more suitable. For the adsorption process, the F value of the model (88.81) with a very small p value (<0.0001) and for the simultaneous adsorption and degradation process, the F value of the model (112.32) with a very small p value (<0.0001) infers that the model is significant and can be used for studying the related between the variables. Also the high coefficient of determination (R^2) and the closeness

of the values of predicted R^2 to adjusted R^2 (they should not have more than 0.2 difference) in the both process indicate that there is a high correlation between the experimental values and predicted response (Samakchi et al. 2018). In addition, the report of lack of fit without p-value can be shown the closeness of the amount of central points. Also, the adsorption and simultaneous adsorption and degradation processes of the results are fitted with quartic (Eq. 5) and cubic (Eq. 6) equations, respectively. It is shown as follows:

$$\%Re = 94.21 + 5.89A - 1.23B - 3.33C - 6.33D - 66.91A^2 - 5.35C^2 - 10.68BC^3 + 54.74A^4 \quad (5)$$

$$\%Re = 80.60 + 4.31A - 47.85E - 10.21A^2 + 3.00C^2 - 14.35B^2C + 14.19B^2D - 11.81A^3 + 8.03B^3 + 66.02E^3 \quad (6)$$

where A is the pH, B is the contact time (min), C is the nano-composite doses (g/min), D is the initial dye concentration (ppm), E is the temperature ($^{\circ}\text{C}$).

The insignificant effect for time and nanocomposite dose is considered (g/L), according to the p value;

Table 6 The factors and results for simultaneous adsorption and degradation process using NTC as P1

Run	Factor 1	Factor 2	Factor 3	Factor 4	Factor 5	Response 1	
	A:pH	B:time	C:C ₀	D:T	E:Dose	Re	
		min	ppm	°C	g/L	%	
						Actual value	Predicted value
1	4	10	10	20	5	93.2721	92.94
2	6	10	10	20	5	93.3852	93.52
3	7	10	10	20	5	98.7232	98.65
4	8	10	10	20	5	95.2454	95.52
5	10	10	10	20	5	78.3012	78.94
6	7	5	10	20	5	83.5217	82.96
7	7	10	10	20	5	96.5212	95.65
8	7	15	10	20	5	97.5231	96.25
9	7	20	10	20	5	99.5412	99.02
10	7	10	5	20	5	98.5212	98.21
11	7	10	10	20	5	98.7232	97.65
12	7	10	15	20	5	93.2512	94.05
13	7	10	20	20	5	94.5123	93.42
14	7	10	30	20	5	95.2352	95.02
15	7	10	10	20	5	98.3252	95.65
16	7	10	10	40	5	99.1242	99.23
17	7	10	10	60	5	99.5212	99.81
18	7	10	10	20	1	63.2124	62.59
19	7	10	10	20	3	85.5212	86.05
20	7	10	10	20	5	98.5295	98.65
21	7	10	10	20	10	83.9852	83.27
22	7	10	10	20	20	99.2561	99.94

Table 7 The ANOVA table for the %Re in alone adsorption process using NTC as P1

Source	Sum of squares	df	Mean square	F value	p value	
Model	545.20	8	68.15	88.81	< 0.0001	Significant
A-pH	77.02	1	77.02	100.37	< 0.0001	
B-time	2.15	1	2.15	2.80	0.1184	
C-m	2.25	1	2.25	2.93	0.1107	
D-C0	121.38	1	121.38	158.18	< 0.0001	
A ²	74.74	1	74.74	97.39	< 0.0001	
C ²	18.18	1	18.18	23.70	0.0003	
BC ³	12.66	1	12.66	16.50	0.0013	
A ⁴	50.88	1	50.88	66.30	< 0.0001	
Residual	9.98	13	0.7674			
Lack of fit	9.98	9	1.11			
Pure error	0.0000	4	0.0000			
Cor total	555.18	21				

however, it can be noticed that these factors have significant effect by the interaction with each others; therefore, they are remained in the equation.

According to the p-value, it can be noticed that the effect of pH is insignificant, but the significant effect for

the square and quartic of this factor is an acceptable reason for considering the pH in the equation. Some of the others statistical data for BG removal in alone adsorption and simultaneous adsorption and degradation processes are shown in Tables 9 and 10.

Table 8 The ANOVA table for the %Re in simultaneous adsorption and photodegradation process using NTC as P1

Source	Sum of squares	df	Mean square	F value	<i>p</i> value	
Model	1570.62	10	157.06	112.32	< 0.0001	Significant
A-pH	3.26	1	3.26	2.33	0.1550	
B-time	118.50	1	118.50	84.74	< 0.0001	
C-C0	18.60	1	18.60	13.30	0.0038	
D-T	14.60	1	14.60	10.44	0.0080	
E-m	652.64	1	652.64	466.73	< 0.0001	
A ²	156.28	1	156.28	111.76	< 0.0001	
C ²	9.60	1	9.60	6.86	0.0238	
B ² C	69.43	1	69.43	49.65	< 0.0001	
A ³	22.05	1	22.05	15.77	0.0022	
E ³	974.78	1	974.78	697.10	< 0.0001	
Residual	15.38	11	1.40			
Lack of fit	15.38	7	2.20			
Pure error	0.0000	4	0.0000			
Cor total	1586.00	21				

Table 9 Statistical data for %Re in alone adsorption process

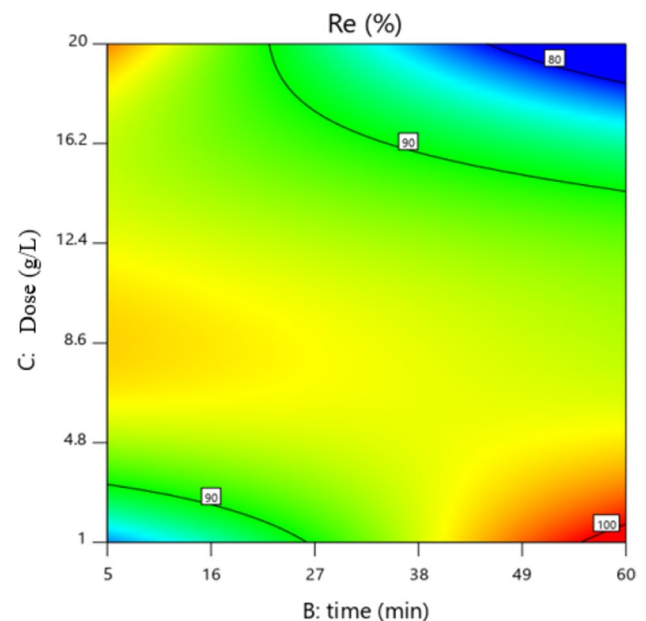
Std. dev	0.8760	R^2	0.9820
Mean	95.46	Adjusted R^2	0.9710
C.V. %	0.9176	Predicted R^2	0.7915
		Adeq precision	35.4625

Table 10 Statistical data for %Re in simultaneous adsorption and degradation process

Std. dev	1.18	R^2	0.9903
Mean	92.00	Adjusted R^2	0.9815
C.V. %	1.29	Predicted R^2	0.7876
		Adeq precision	44.5520

B Data interpretation for the adsorption process using NTC

The contour and 3D plots those are shown sequential, noticing the effect of varying adsorbent dosage (g/L) and contact times (min). The pH, initial dye concentration and temperature were fixed at their center points (pH = 7, $C_0 = 22.5$ ppm and $T = 23.5$ °C, respectively). As can be seen from Figs. 6 and 7, the percent of dye removal (%Re) increases with the increase in adsorbent dosage in the lower times and with the decreases in adsorbent dosage in the higher times. By increasing the adsorbent dosage, the activated sites for adsorption will be increased; in the other hand, desorption of dye from the adsorbent surface can be the cause for decreasing this process.

**Fig. 6** The contour plot for the interaction of adsorbent dosage (g/L) and contact times (min) in the fixed points of pH=7, $C_0 = 22.5$ ppm and $T = 23.5$ °C for the alone adsorption process

The predicted data by RSM versus experimental data for adsorption process are shown in Fig. 8. It is investigated that the predicted and experimental data are in good agreement with each other and it can be shown that the RSM could successfully predict the removal percentage through the adsorption process.

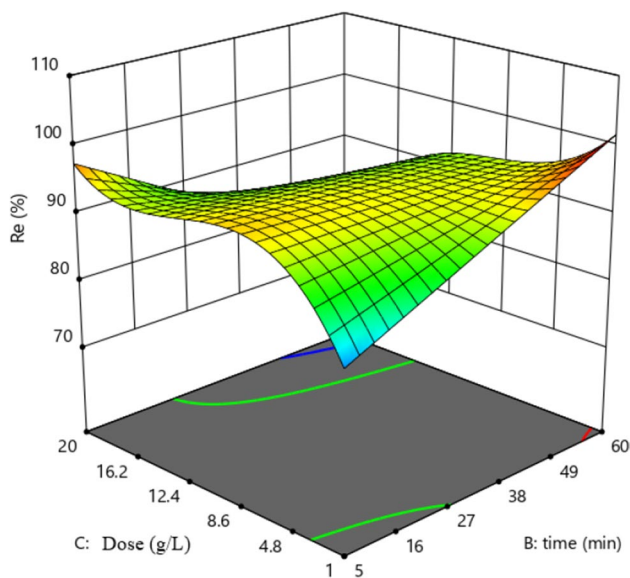


Fig. 7 The 3D plot for the interaction of adsorbent dosage (g/L) and contact times (min) in the fixed points of pH=7, $C_0=22.5$ ppm and $T=23.5$ °C for the alone adsorption process

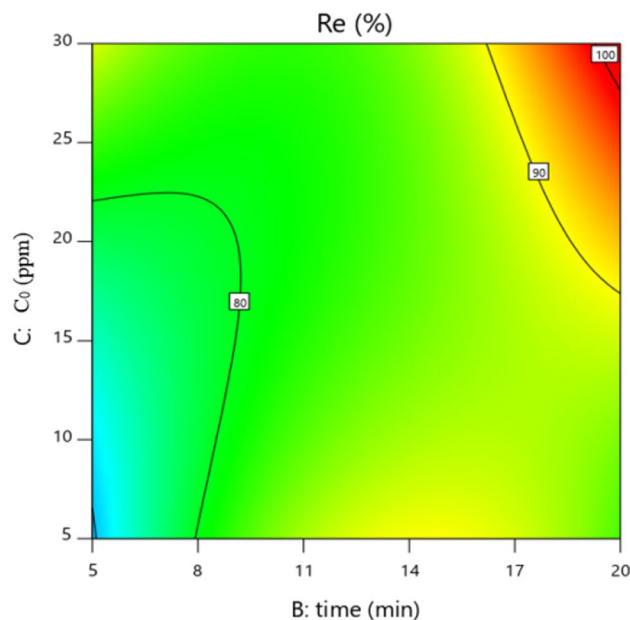


Fig. 9 The contour plot for the interaction of contact times (min) and initial dye concentration (ppm) in the fixed points of pH=7, $T=40$ °C and dose=10.5 g/L for the simultaneous adsorption and photodegradation process

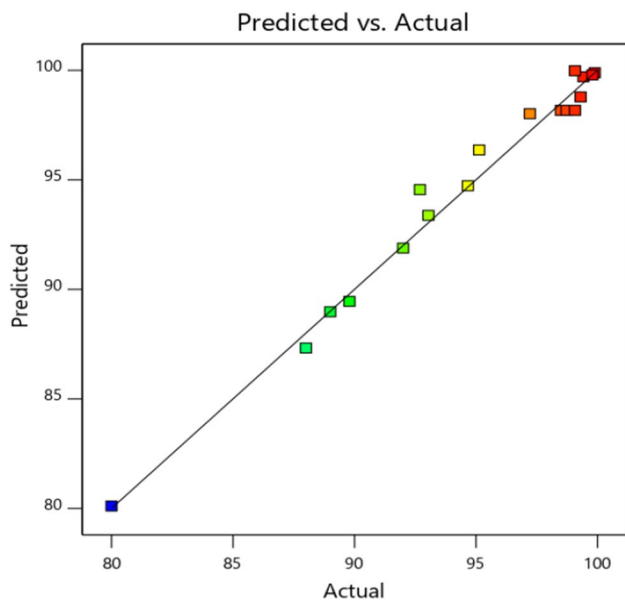


Fig. 8 Actual data obtained by experiments versus predicted data for the alone adsorption process

C Data interpretation for simultaneous adsorption and photodegradation processes

The interaction of time (min) and initial dye concentration (ppm) on this process is illustrated by the contour and 3D plots which are shown sequential in Figs. 9 and 10 The pH, temperature and dosage were fixed at their center

points (pH=7, $T=40$ °C and dose = 10.5 g/L, respectively). The dye simultaneous adsorption and degradation process increases during time with the lower amounts of initial dye concentration, and it can be happened due to the cause of the more effect of UV light in degradation process. Also in the higher dye concentration, the more molecules movement can be a motivation for adsorption process, and duo to the effect of this process on the degradation, the removal efficiency will be increased.

The predicted data by RSM versus experimental data for adsorption process are shown in Fig. 11. It is investigated that the predicted and experimental data are in good agreement with each other and it can be shown that the RSM could successfully predict the removal percentage through the adsorption process.

D Optimal conditions for the alone adsorption (AA) and simultaneous adsorption and degradation processes (SAP)

In order to investigate the optimum condition of the parameters to obtain the maximum %Re during the adsorption and simultaneous adsorption and degradation processes, i the desirability function of the software is used, which was set for the response of maximum (% 100) to achieve the highest removal efficiency percentage (Habibzadeh et al. 2018). For the adsorption process, the highest dye removal (% 99) was predicted under condition of pH = 6.9, contact

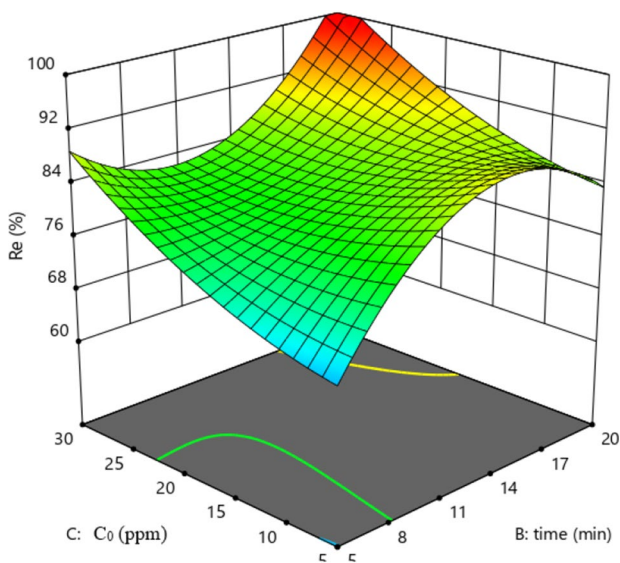


Fig. 10 The 3D plot for the interaction of contact times (min) and initial dye concentration (ppm) in the fixed points of $\text{pH}=7$, $T=40\text{ }^{\circ}\text{C}$ and dose = 10.5 g/L for the simultaneous adsorption and photodegradation process

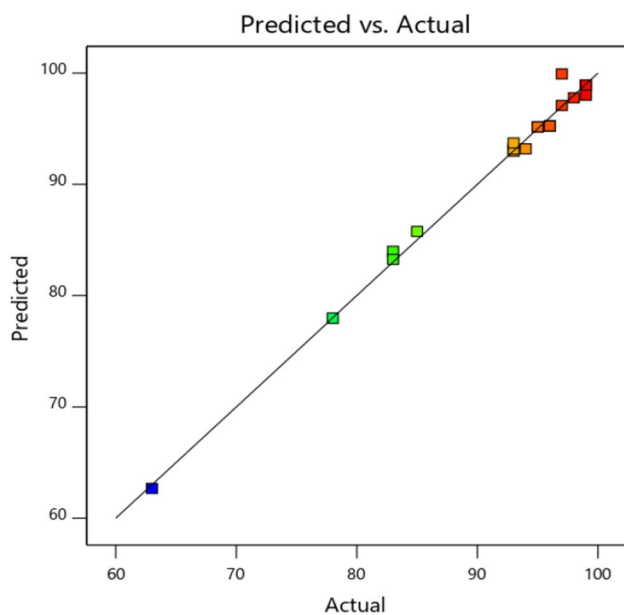


Fig. 11 Actual data obtained by experiments versus predicted data for the simultaneous adsorption and degradation process

time = 19.3 min , dosage = 6.2 g/L , initial dye concentration (C_0) = 6 ppm and temperature = $23.5\text{ }^{\circ}\text{C}$. The maximum experimental removal efficiency by this process was calculated % 99.884 .

In addition by the same software, the highest dye removal (% 99.4) during the simultaneous adsorption and photodegradation processes occurred in $\text{pH}=7.6$,

time = 9.8 min , dosage = 6.3 g/L , initial dye concentration (C_0) = 6 ppm and temperature = $30\text{ }^{\circ}\text{C}$.

Conclusions

This study was carried out to consider the removal of BG dye using the synthesized ($\alpha\text{-Fe}_2\text{O}_3\text{NPs/lemon peel (LP)/Fe}_3\text{O}_4\text{NPs}$) nanobiocomposite, simultaneously and separately with the removal process during the simultaneous adsorption and photodegradation, and alone adsorption processes in the batch and fixed bed systems. The more stabilization and agglomeration of NPs were studied due to SAP and AA, respectively, for simultaneous synthesis and removal process in the batch unit by XPS and TEM results.

It was confirmed for the first time that the highest total removal and adsorption efficiency of a dye by a nanobiocomposite occur when the final stages of synthesis and growth of its nanoparticles are accompanied by simultaneous adsorption and photodegradation (SAP) due to autocatalytic role of small organic substances obtained from photodegradation of BG in stabilization and higher efficiency of nanoparticles of ($\alpha\text{-Fe}_2\text{O}_3\text{NPs/lemon peel (LP)/Fe}_3\text{O}_4\text{NPs}$) in batch system. So that adsorption of BG by NPs was increased several times (713%) compared with that of separate synthesis and removal. Also, the total removal of BG increased from 80.8% by the nanobiocomposite synthesized separately from removal process in AA to 99.6% by the nanobiocomposite synthesized simultaneously with removal process in SAP.

Funding The author(s) received no specific funding for this work

Declarations

Conflict of interest The authors whose names are listed immediately below certify that they have NO affiliations with or involvement in any organization or entity with any financial interest (such as honoraria, educational grants, participation in speakers' bureaus; membership, employment, consultancies, stock ownership, or other equity interest; and expert testimony or patent-licensing arrangements), or non-financial interest (such as personal or professional relationships, affiliations, knowledge or beliefs) in the subject matter or materials discussed in this manuscript. This statement is signed by all the authors to indicate agreement that the above information is true and correct.

Open Access This article is licensed under a Creative Commons Attribution 4.0 International License, which permits use, sharing, adaptation, distribution and reproduction in any medium or format, as long as you give appropriate credit to the original author(s) and the source, provide a link to the Creative Commons licence, and indicate if changes were made. The images or other third party material in this article are included in the article's Creative Commons licence, unless indicated otherwise in a credit line to the material. If material is not included in the article's Creative Commons licence and your intended use is not permitted by statutory regulation or exceeds the permitted use, you will need to obtain permission directly from the copyright holder. To view a copy of this licence, visit <http://creativecommons.org/licenses/by/4.0/>.

References

- Ahmad A, Hameed B (2010) Fixed-bed adsorption of reactive azo dye onto granular activated carbon prepared from waste. *J Hazard Mater* 175:298–303. <https://doi.org/10.1016/j.jhazmat.2009.10.003>
- Ahmmad B (2013) Green synthesis of mesoporous hematite (α -Fe₂O₃) nanoparticles and their photocatalytic activity. *Adv Powder Technol* 24:160–167. <https://doi.org/10.1016/j.apt.2012.04.005>
- Cędrowska E, Pruszyński M, Gawęda W, Żuk M, Krysiński P (2020) Conjugated superparamagnetic iron oxide nanoparticles labeled with 225Ac as a perspective tool for combined α -radioimmunotherapy and magnetic hyperthermia of HER2-positive breast cancer. *Molecules* 25:1025–1032. <https://doi.org/10.3390/molecules25051025>
- Duxbury DF (1993) The photochemistry and photophysics of triphenylmethane dyes in solid and liquid media. *Chem Rev* 93:381–433. <https://doi.org/10.1021/cr00017a018>
- Eshaghi Z, Ahmadi-Kalateh Khooni M (2011) Determination of brilliant green from fish pond water using carbon nanotube assisted pseudo stir-bar solid/liquid microextraction combined with UV-vis spectroscopy-diode array detection. *Spectrochim Acta Part A* 79(3):603–607. <https://doi.org/10.1016/j.saa.2011.03.042>
- Habibzadeh M, Chaibakhsh N, Naeem AS (2018) Optimized treatment of wastewater containing cytotoxic drugs by living and dead biomass of the freshwater microalga, *Chlorella vulgaris*. *Ecol Eng* 111:85–93. <https://doi.org/10.1016/j.ecoleng.2017.12.001>
- Liu Q, Tang J, Li X, Lin Q, Xiao R, Zhang M, Yin G, Zhou Y (2020) Effect of ignosulfonate on the adsorption performance of hematite for Cd(II). *Sci Total Environ* 738:139952. <https://doi.org/10.1016/j.scitotenv.2020.139952>
- Mohammadi A, Daemi H, Barikani M (2014) Fast removal of malachite green dye using novel superparamagnetic sodium alginate-coated Fe₃O₄ nanoparticles. *Int J Biol Macromol* 69:447–455. <https://doi.org/10.1016/j.ijbiomac.2014.05.042>
- Mohnen D (2008) Pectin structure and biosynthesis. *Curr Opin Plant Biol* 11(3):266–277. <https://doi.org/10.1016/j.pbi.2008.03.006>
- Oboh G, Olashinde T, Ademosun A (2014) Essential oil from lemon peels inhibit key enzymes linked to neurodegenerative conditions and pro-oxidant induced lipid peroxidation. *J Oleo Sci* 63(4):373–381. <https://doi.org/10.5650/jos.ess13166>
- Rakhshae R, Darvazeh J (2017) Comparing performance of three forms of hematite in fixed bed reactor for a photocatalytic decolorization: experimental design, model fitting and optimization of conditions. *Process Saf Environ Prot* 107:122–137. <https://doi.org/10.1016/j.psep.2017.02.006>
- Rakhshae R, Darvazeh J (2018) Studying role of air bubbles on suspension of hematite particles with three size ranges in plug flow reactor to improve dyes photo degradation compared to conventional packed bed photo reactors. *J Hazard Mater* 356:61–67. <https://doi.org/10.1016/j.jhazmat.2018.05.025>
- Rakhshae R, Noorani Y (2017) Comparing three methods of simultaneous synthesis and stabilization of Fe₃O₄ nanoparticles: changing physicochemical properties of products to improve kinetic and thermodynamic of dye adsorption. *J Magn Magn Mater* 422:128–140. <https://doi.org/10.1016/j.jmmm.2016.08.078>
- Rivas-Cantu R, Jones KD, Mills PL (2013) A citrus waste-based biorefinery as a source of renewable energy: technical advances and analysis of engineering challenges. *Waste Manage Res* 31(4):413–420. <https://doi.org/10.1177/0734242X13479432>
- Samakchi S, Chaibakhsh N, Moradi-Shoeili Z (2018) Synthesis of MoS₂/MnFe₂O₄ nanocomposite with highly efficient catalytic performance in visible light photo-Fentonlike process. *J Photochem Photobiol A* 367:420–428. <https://doi.org/10.1016/j.jphotochem.2018.09.003>
- Seshadri S, Bishop PL, Agha AM (1994) Anaerobic/aerobic treatment of selected azo dyes in wastewater. *Waste Manage* 14(2):127–137. [https://doi.org/10.1016/0956-053X\(94\)90005-1](https://doi.org/10.1016/0956-053X(94)90005-1)
- Toor AP (2006) Photocatalytic degradation of Direct Yellow 12 dye using UV/TiO₂ in a shallow pond slurry reactor. *Dyes Pigments* 68:53–60. <https://doi.org/10.1016/j.dyepig.2004.12.009>
- Wang YN, Gao F, Liu T, Hou Y, Zhu Y, Ye W, Wang L (2016) Effects of self-assembly of 3-phosphonopropionic acid, 3-aminopropyltrimethoxysilane and dopamine on the corrosion behaviors and biocompatibility of a magnesium alloy. *Mater Sci Eng C* 67:132–143. <https://doi.org/10.1016/j.msec.2016.05.038>
- Yagub MT (2014) Dye and its removal from aqueous solution by adsorption: a review. *Adv Colloid Interface Sci* 209:172–184. <https://doi.org/10.1016/j.cis.2014.04.002>
- Zamani H, Rakhshae R, Garakoui SR (2018) Two contrary roles of Fe₃O₄ nanoparticles Rashtia immobilized on sodium alginate gel beads. *J Hazard Mater* 344:566–575. <https://doi.org/10.1016/j.jhazmat.2017.10.061>
- Zhang K, Xie R, Fang K, Chen W, Shi Z, Ren Y (2019) Effects of reactive dye structures on surface tensions and viscosities of dye solutions. *J Mol Liq* 287:110932. <https://doi.org/10.1016/j.molliq.2019.110932>

Publisher's Note Springer Nature remains neutral with regard to jurisdictional claims in published maps and institutional affiliations.